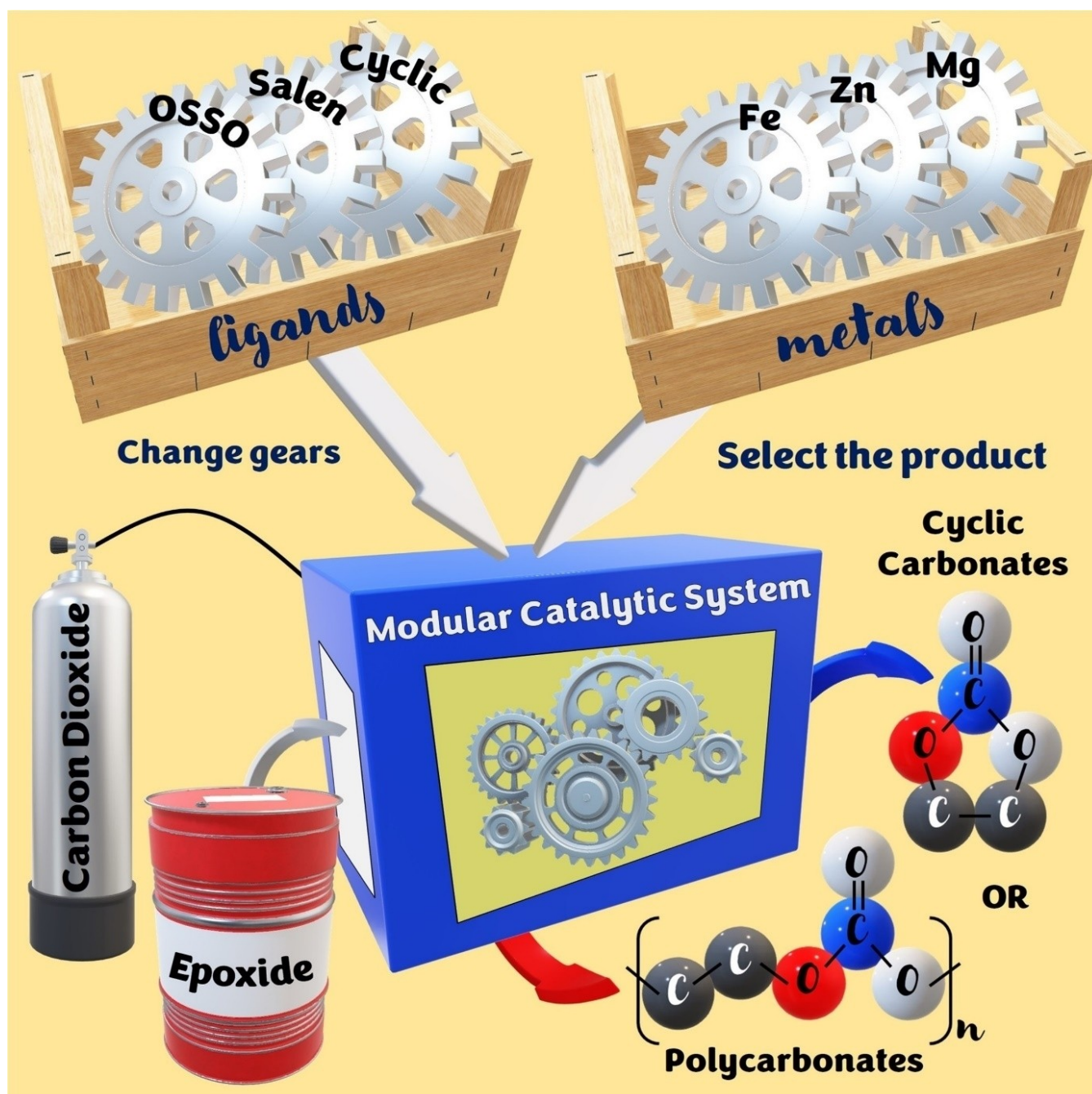


# Recent Advancements in Metal-catalysts Design for CO<sub>2</sub>/Epoxide Reactions

Francesco Della Monica<sup>\*[a]</sup> and Carmine Capacchione<sup>\*[b]</sup>



**Abstract:** Carbon dioxide utilization is considered an effective strategy to mitigate the carbon footprint of chemical industry. Among other uses, the incorporation of carbon dioxide into cyclic organic carbonates (COCs) and aliphatic polycarbonates (APCs) has received great attention in the field of homogeneous catalysis. After few decades of research activity, a wide range of metal-based catalytic systems has been reported to promote this reaction. Nonetheless, a better

comprehension of the apparently simple reaction mechanism of such transformations has been reached only in recent years. This, in turn, allowed for the design of new catalytic systems guided by a clearer mechanistic picture. In this review, we present the most recent advancements in this field, distinguishing between catalysts for COCs and APCs production classified on the bases of their ligand structures.

## 1. Introduction

Carbon dioxide utilization (CDU) has become an intensive task of research because of the possibility to obtain useful products from a molecule considered the major responsible for the greenhouse effect.<sup>[1,2,3]</sup> Actually, the interest in using CO<sub>2</sub> arises not only with the aim to reduce its concentration in the atmosphere but also from the fact that CO<sub>2</sub> is a favorable alternative, in terms of availability, cost, and toxicity, to other C1 sources such as carbon monoxide and phosgene.<sup>[4]</sup> These advantages, however, oppose to two major drawbacks: the thermodynamic stability and the kinetic inertness of the CO<sub>2</sub> molecule.

In such scenario, the reaction of CO<sub>2</sub> with epoxides represents one of the most studied reactions not only because of the possibility to react CO<sub>2</sub> with high reactive molecules but also because of the possibility, by regulating the reaction conditions and with a wise choice of the catalytic system, to obtain two useful products: cyclic organic carbonates (COCs) and aliphatic polycarbonates (APCs).<sup>[5–14]</sup>

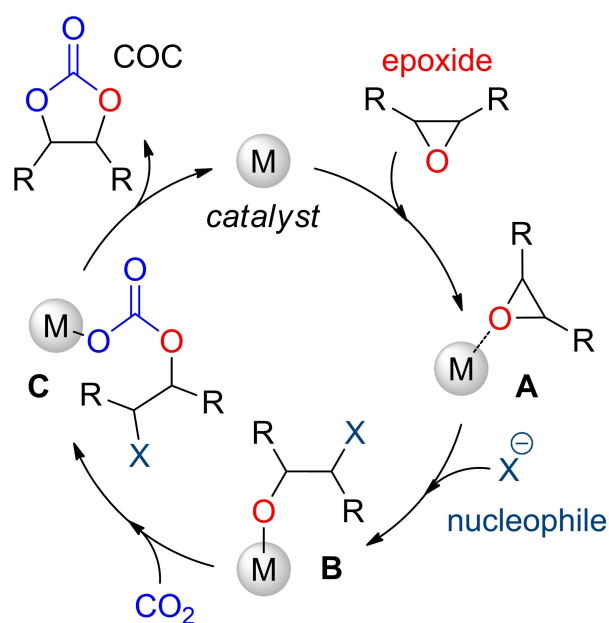
Notwithstanding the general trend to limit the use of metal centers in catalysis,<sup>[15–17]</sup> homogeneous catalytic systems based on metal complexes still offer the best option in terms of activity, selectivity, and mild reaction conditions. In this contribution we report the last advancements in the design of metal-catalyzed synthesis of cyclic carbonates and polycarbonates highlighting the new approaches conceived in the last three years of activity in these field.

## 2. Cyclic Organic Carbonates

Cyclic organic carbonates constitute an important class of molecules that have several commercial applications as green polar aprotic solvents,<sup>[18]</sup> electrolytes in Li-ion batteries,<sup>[19]</sup> monomers for the production of polycarbonates,<sup>[20]</sup> and valuable synthetic building block for the synthesis of fine chemicals.<sup>[21]</sup>

Indeed, the industrial synthesis of COCs that was initially based on the reaction between diols and phosgene shifted to the more sustainable and 100% atom efficient cycloaddition of CO<sub>2</sub> to epoxides. At the industrial scale, this reaction is performed by using tetra-alkylammonium halide (namely tetraethylammonium bromide) that furnish the suitable nucleophile for the ring-opening of the epoxide (see Scheme 1). Notably, even the more reactive substrates such as ethylene oxide (EO) and propylene oxide (PO) require high temperatures ( $\geq 100$  °C) and high catalyst loading.

In this field, the endeavors to find more active catalytic systems followed, in the last years, many routes spanning from heterogeneous catalytic systems based on metal oxides and MOF,<sup>[22,23]</sup> organocatalysts based on ionic liquids,<sup>[24,25]</sup> or hydro-



**Scheme 1.** Generally proposed mechanism for the formation of COCs catalyzed by a metal complex and a nucleophile.

[a] Dr. F. Della Monica  
Dipartimento di Biotecnologie e Scienze della Vita  
Università degli Studi dell'Insubria  
Via J. H. Dunant 3,  
21100 – Varese (Italy)  
E-mail: f.dellamonica@uninsubria.it

[b] Prof. Dr. C. Capacchione  
Dipartimento di Chimica e Biologia “Adolfo Zambelli”  
Università degli Studi di Salerno  
Via Giovanni Paolo II,  
84084 – Fisciano, SA (Italy)  
E-mail: c.capacchione@unisa.it

This manuscript is part of a special collection on Carbon Dioxide Utilization in Organic Chemistry.

© 2022 The Authors. Asian Journal of Organic Chemistry published by Wiley-VCH GmbH. This is an open access article under the terms of the Creative Commons Attribution License, which permits use, distribution and reproduction in any medium, provided the original work is properly cited.

gen-bond donors (HBDs),<sup>[16,26]</sup> and binary systems formed by the combination of a metal complex and an onium salt.<sup>[13,27]</sup> In the latter case the Lewis acidic metal center (M, Scheme 1) activates the epoxide (A) and the onium salt furnishes the nucleophile X<sup>-</sup> (generally a halide anion Cl<sup>-</sup>, Br<sup>-</sup> or I<sup>-</sup>) that causes the ring-opening of the substrate and allows the insertion of the CO<sub>2</sub> into the metal-alkoxo bond (B) with the formation of an hemicarbonato species (C) that evolves to the ring-closing. In some cases the metal center also activates the CO<sub>2</sub> further lowering the activation energy of the overall process.

Despite the intrinsic complication of using a metal-based binary catalytic system this approach offers, in general, higher activity and wider substrate scope compared to other catalytic systems (e.g., organocatalysts) and, as for other homogeneous catalysts, the possibility to fine tune the steric and electronic properties of the metal center by judicious choice of the ancillary ligand. Notwithstanding a high level of performance

has been reached, in the last years particular attention has been paid to the following points:

- development of catalysts based on Earth-crust abundant and non-toxic metals (Ti, Fe, Al, Zn);<sup>[12,28]</sup>
- shifting from binary to single component catalysts also by using bimetallic or multimetallic systems.
- in-depth comprehension of the mechanistic aspects also by using DFT calculations.

Here we report on the last developments in this field distinguishing between COCs and APCs production and classifying the catalytic systems on the basis of the ligand framework.

## 2.1. Salen and salen-like ligands

The ease of synthesis and the possibility to form complexes with, virtually, all kind of metal centers render the salen ligands the ideal candidates to develop active catalysts for the CO<sub>2</sub>/epoxide reaction.<sup>[29]</sup> As a matter of fact, these tetradentate ligands offer a scaffold that can be simply tuned by changing the type of the bridge between the nitrogen atoms and the steric bulk of the R<sub>1</sub>, R<sub>2</sub> substituents (Scheme 2).

Furthermore, a series of related ligands containing Schiff-bases have been developed to further vary the electronic and steric features of the metal center. In the CO<sub>2</sub>/epoxide cycloaddition, tetradentate salen ligands have already shown to perform very well with many metal centers such as Al, Zn, Fe, Cr but their potential for the possibility of obtaining new ligand structures has been not completely expressed.

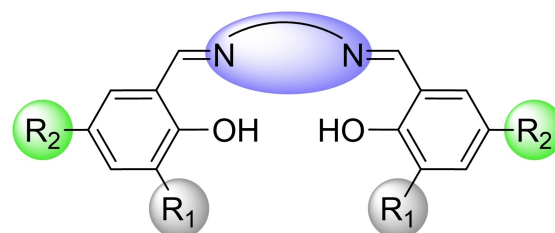
In 2021 Phomphrai and coworkers reported a new family of constrained geometry salen ligands (inden-ligands) that forces the N and O coordinating atoms to be coplanar with the aromatic ring, resulting in a more rigid coordinating environment for the metal center.<sup>[30]</sup> In particular the Cr(III) complex **1** in the presence of TBAB catalyzes the cycloaddition of CO<sub>2</sub> to PO with higher TOF (1900 h<sup>-1</sup>) compared to a regular ethylene-bridged salen Cr(III) complex **2** (1250 h<sup>-1</sup>) under the same reaction conditions (80 °C, 2.1 MPa of CO<sub>2</sub>, 1 h) (Figure 1).

DFT calculations explain this difference in activity with a lower barrier for the CO<sub>2</sub> insertion for the complex **1** vis-à-vis **2**. By increasing the monomer/cocatalyst/catalyst ratios up to 20000/200/1 a TOF up to 14800 h<sup>-1</sup> was achieved for PO. Other terminal epoxides also give good result with high TOF (e.g., up to 16600 h<sup>-1</sup> for epichlorohydrin). When using internal epoxides as the substrates, namely cyclopentene oxide (CPO) and cyclohexene oxide (CHO), lower activities were observed (TOF of 390

Francesco Della Monica gained his M.Sc. (2013) and PhD in Chemistry (2018) at the University of Salerno (Italy) under the supervision of Prof. Carmine Capacchione. His work was focussed on the development of new Fe-based catalysts for CO<sub>2</sub>/epoxides reactions. As postdoctoral researcher at the same institute, he became interested in the green, catalytic synthesis of value-added products from renewables. In 2019, he joined the group of Prof. Arjan W. Kleij at the Institute of Chemical Research of Catalonia (Spain) with a Marie Skłodowska-Curie Individual Fellowship to develop new terpenoid monomers for the synthesis of sustainable polymers. In 2022, he joined the Department of Biotechnology and Life Science of the University of Insubria (Italy) as assistant professor. His research is currently directed to the catalytic valorisation of carbon dioxide and bio-based building-blocks in sustainable (polymer) chemistry.



Carmine Capacchione received his M.Sc. and PhD degrees from the University of Salerno (Italy) under the supervision of Antonio Proto. He then held an Alexander von Humboldt post-doctoral fellowship working at the University of Heidelberg (Germany) in the group of Lutz H. Gade. He was appointed assistant professor in 2005 and promoted to associate professor in 2015 at the University of Salerno (Italy). From 2021 he is full professor at the same institute. His research interest is in the field of homogeneous catalysis with a focus on the valorisation of bio-based feedstock and CO<sub>2</sub> utilization.



Scheme 2. General structure of a salen ligand.

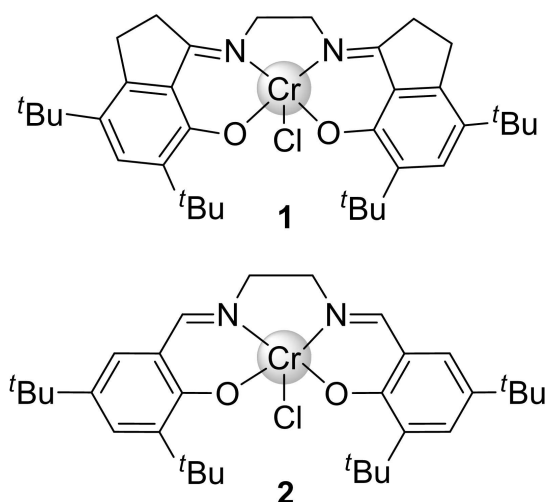


Figure 1. Structure of inden-Cr complex 1 and salen-Cr complex 2.

and  $168 \text{ h}^{-1}$ , respectively). This is likely due to the higher steric hindrance hampering the ring-opening step. In addition, CHO yields a mixture of cyclic and polymeric products, with a COC:PC ratio equal to 64:36.

In this kind of catalysis, the formation of different products depending on reaction conditions is a phenomenon known from long time ago.<sup>[31–39]</sup> Working with salen-Cr complexes, Darensbourg demonstrated that this dependence is due to different activation barriers for the back-biting and propagation steps, resulting in possible kinetic or thermodynamic control depending on the reaction temperature employed.<sup>[40]</sup> This scenario has been confirmed in the case of bimetallic Zn complexes.<sup>[41]</sup> However, a more complex mechanistic scenario was proposed for structurally related salen-Cr,<sup>[42]</sup> and [OSSO]-Fe catalysts.<sup>[43]</sup> Recently, this topic has been extensively discussed.<sup>[44]</sup>

Titanium(IV) 3 (forming a bimetallic  $\mu$ -oxo bridged structure in the solid state) and Vanadium(V) 4 complexes have been also reported by North and coworkers to catalyze the conversion of styrene oxide (SO) to styrene carbonate (SC) under a wide-range of reaction conditions (0.1–5 MPa; 25–100 °C, 3–24 h) reaching a conversion of 98% conversion in 24 h by activation with TBAB (Figure 2).<sup>[45]</sup> Other terminal epoxides have been also converted to cyclic carbonates in good yields, while CHO only gives the corresponding *cis*-cyclohexene carbonate (*cis*-CHC) in low yields (23–32% with the titanium and vanadium catalysts respectively). Notably, despite both the metal complexes are chiral, SO is converted in the corresponding carbonate in the racemic form.

The results were rationalized through DFT calculations showing that the metal center acts as Lewis bases activating the  $\text{CO}_2$  rather than as Lewis acid activating the epoxide ring as commonly accepted. The consequently proposed catalytic cycle is depicted in Scheme 3. The role of the bromine, borne by TBAB, that is not directly involved in the catalytic cycle, is supposed to coordinate to the metal center forming a pentacoordinated species with enhanced Lewis basicity.

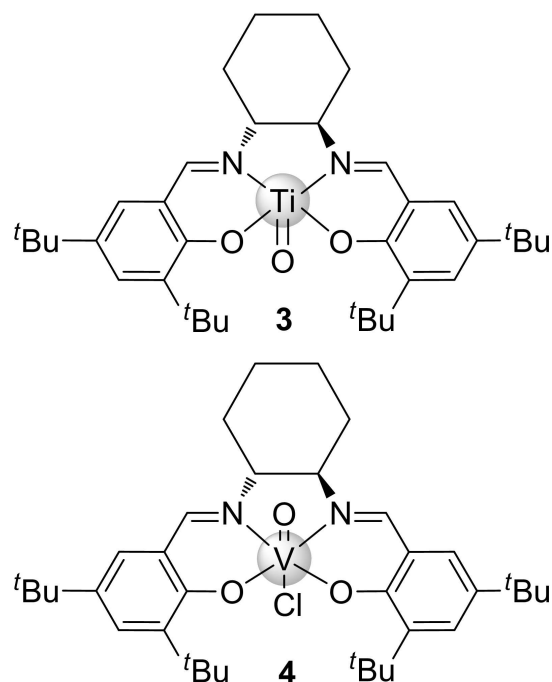
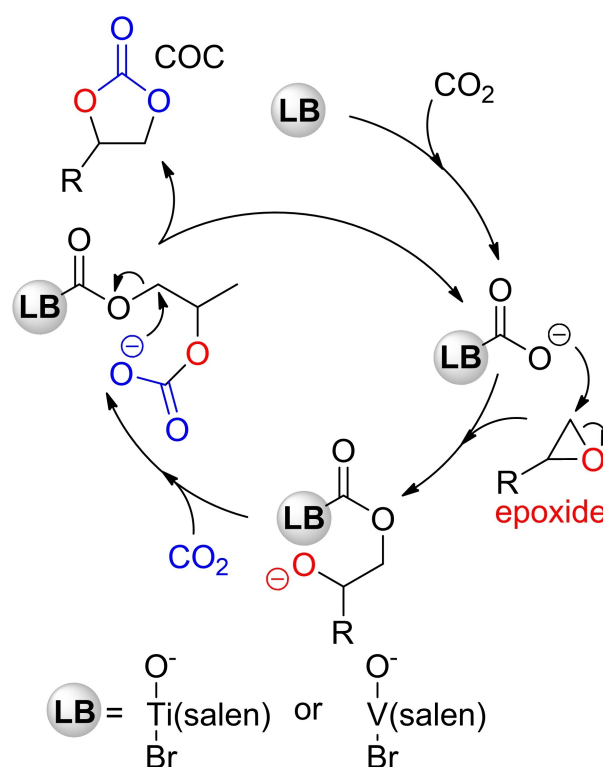


Figure 2. Structure of salen-Ti 3 and salen-V 4 complexes.



Scheme 3. Proposed reaction mechanism for the formation of cyclic carbonates catalyzed by 3 and 4 upon reaction with TBAB.

Lately Mn(II), 5 Fe(II) 6 and Co(II) 7 and 8 complexes bearing a tridentate Schiff-base ONO-ligand were reported by Viciano and coworkers to catalyze the cycloaddition of  $\text{CO}_2$  to PO with moderate activity in the presence of bis-(triphenylphosphine)-

iminium chloride (PPNCl) as co-catalyst (Figure 3).<sup>[46]</sup> Under optimized reaction conditions (3 MPa, 80 °C, 1 h), in the presence of 2 equivalents of TBAB, the Mn(II) complex **5** can reach a TOF of 1600 h<sup>-1</sup>.

The Co(III) complex **9** bearing a ONN Schiff-base ligand was also reported by Larion (Figure 4).<sup>[47]</sup> In this case the design of the metal complexes is based on the concept of increasing the hydrogen bond donor (HBD) ability of the ligand framework being the metal center not involved in the activation of the substrate. Furthermore, the presence of the iodine atoms that acts as nucleophile allows the use of this complex as single

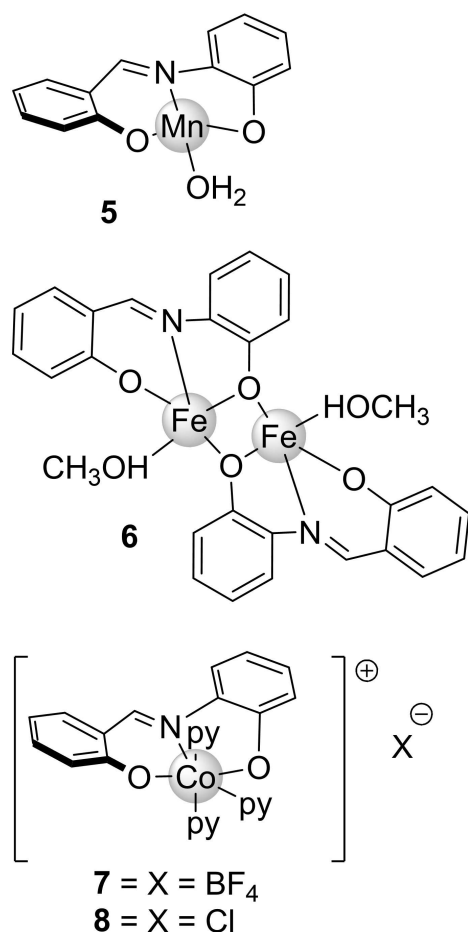


Figure 3. Structure of tridentate ONO-ligand based complexes **5**, **6**, **7** and **8**.

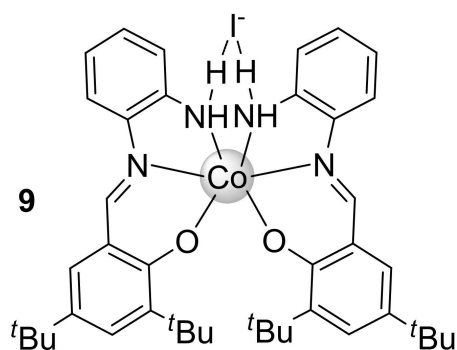


Figure 4. Structure of tridentate ONN-ligand based Co-complex **9**.

component catalyst. Indeed, SO reach a conversion of 90% to the corresponding carbonate in 24 hours under mild reaction conditions (0.1 MPa; 40 °C). Comparison with known hydrogen bond donor (HBD) organocatalysts show the superior performance of this system with TON (up to 38) and TOF (up to 1.6 h<sup>-1</sup>) doubling the highest data reported in the literature. The Co(III) complex **9** also promotes the conversion of other terminal epoxides under mild reaction conditions (0.1 MPa; 40 °C, 24 h). Intriguingly, on one hand the addition of a substoichiometric amount (0.5 equiv.) of ethanol or water to the reaction system resulted in an improvement of the yield, on the other hand an excess of ethanol, water or dimethyl sulfoxide causes a severe drop of the yield. This phenomenon was explained considering the free energies of the adducts formed between SO and the additives. As a matter of fact, ethanol, water, and dimethyl sulfoxide, when present in excess, function as competitive inhibitors preventing the activation of the substrate via hydrogen-bond. The strength of the hydrogen bond between complex **9** and the various additives/substrates was also studied via <sup>1</sup>H NMR confirming the trend obtained in the DFT calculations. Coherently, the mechanistic scenario highlights the ring-opening of the epoxide as rate determining step.

DFT calculations have been extensively used to study the mechanism of the CO<sub>2</sub>/epoxides coupling by using metal-salen complexes by Poater and coworkers.<sup>[48]</sup>

In particular, the authors focused their attention on monomeric salen complexes of Co, Cr, Y and Sc (**10–17**, Figure 5) in the cycloaddition of CO<sub>2</sub> to commercially relevant epoxides such as PO and epichlorohydrin (ECH). This study shows the importance in the choice of the metal center for the obtaining of high active catalysts.

Metals such as Cr, Co and Sc show the same behavior with the CO<sub>2</sub> insertion as the rate limiting step; conversely Y, thanks to its structural features with a larger bite-angle, facilitates the formation of the CO<sub>2</sub> adduct and therefore in this case the most energy demanding step is the COC ring-closure.

DFT calculations were also used to study the behavior of bifunctional metal-salen catalysts with cationic arms (**18–25**, Figure 6).<sup>[49]</sup> Considering Al salen complexes with various cationic arms the most efficient in term of catalytic activity are

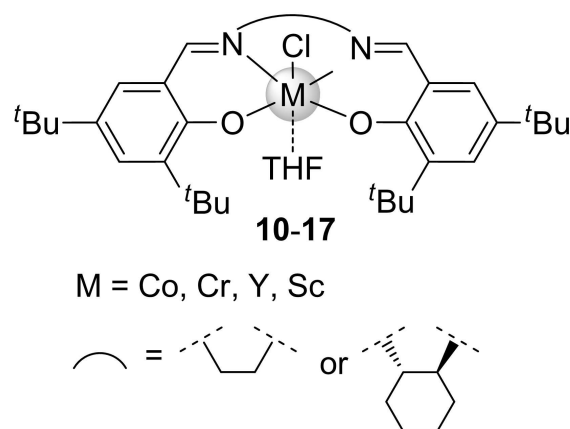


Figure 5. Structures of metal-salen complexes **10–17**.

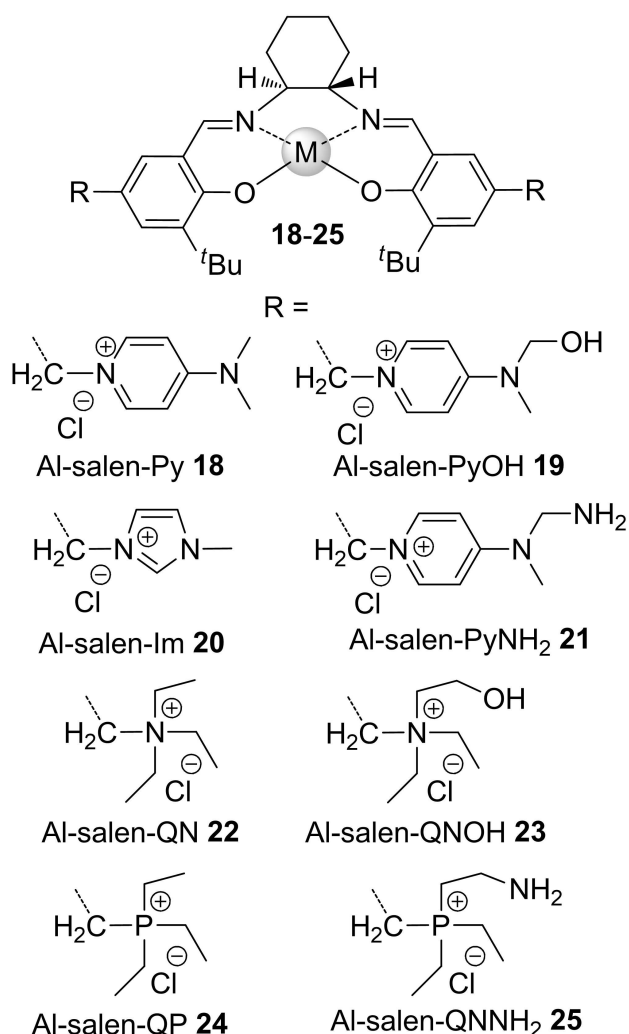


Figure 6. Structures of bifunctional metal-salen complexes 18–25.

the complex **22** and **23**. It is proposed that with this system the rate determining step is the ring-opening of the epoxide activated by the metal center. The authors also studied the effect of the various metal center on the activity, predicting the following order:  $\text{Co(III)} > \text{Cr(III)} > \text{Zn(II)} \approx \text{Al(III)} > \text{Mn(III)}$ . This trend correlates well with the bond distance between the metal ion and the oxygen atom of PO in the reaction complexes. Computations also underline that the metal ion plays a pivotal role in determining the catalytic activity vis-à-vis the type of ionic liquid present in the cationic arms.

The dinuclear iron(III) complex **26** supported by a cyclic salen-type ligand have been also studied through DFT calculations evidencing in this case a different behavior with or without the presence of a cocatalyst (TBAC) (Figure 7).<sup>[50]</sup>

As a matter of fact, in the absence of the external nucleophile a bimetallic, concerted mechanism is operative with the chlorine atom of the second metal center involved in the ring-opening of the epoxide activated on the first metal center, conversely, in the presence of the cocatalyst only one metal center is active in the catalytic cycle. The catalytic cycle in the presence of external nucleophile is energetically favored

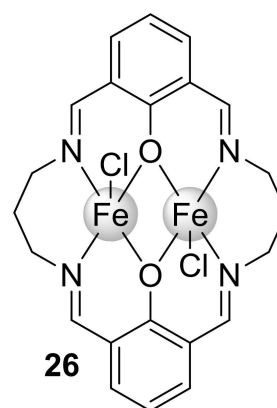
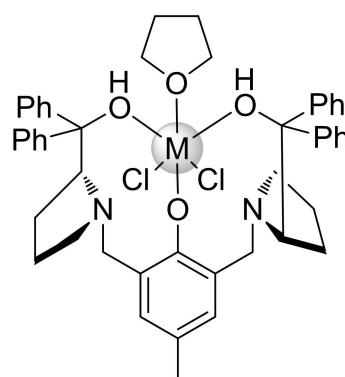


Figure 7. Structures of dinuclear iron(III) complex **26**.

respect to the bimetallic mechanism and therefore is the only one active in the presence of the cocatalyst.

Amino-phenolate ligands were also explored as possible scaffolds for many metal centers in the  $\text{CO}_2$ /epoxide coupling. Zhao and coworkers reported on the use of rare earth metal complexes supported by a Trost ligand (**27–31**, Figure 8).<sup>[51]</sup> The metals are six-coordinated with the nitrogen ligands not included in the coordination sphere. When activated by two equivalents of TBAB these complexes are active in the cycloaddition of  $\text{CO}_2$  to epichlorohydrin with the Sm complex showing the highest activity (65% conversion 0.1 MPa; 25 °C, 24 h). It is worth to note that rising the temperature up to 70 °C a complete conversion for ECH was achieved and a wide range of terminal epoxides can be converted to the corresponding cyclic carbonates. The conversion of internal and disubstituted epoxides was also possible, in this case, by increasing the pressure at 0.7 MPa.

Amino-bridged bis(phenolato) Co(II) complexes **32–34** were reported by Yao and coworkers (Figure 9).<sup>[52]</sup> Furthermore by addition of alkali compounds (KOAc, NaOMe) they observed the formation of multinuclear homometallic species with mixed valence Co(II/III) and M(I) ( $M = \text{Na}$  or  $\text{K}$ ) **35** due to the oxidation



$M = \text{Sm}$  (**27**);  $\text{Eu}$  (**28**);  $\text{Y}$  (**29**);  $\text{Yb}$  (**30**);  $\text{Lu}$  (**31**)

Figure 8. Structures of rare earth metal complexes **27–31** supported by a Trost ligand.

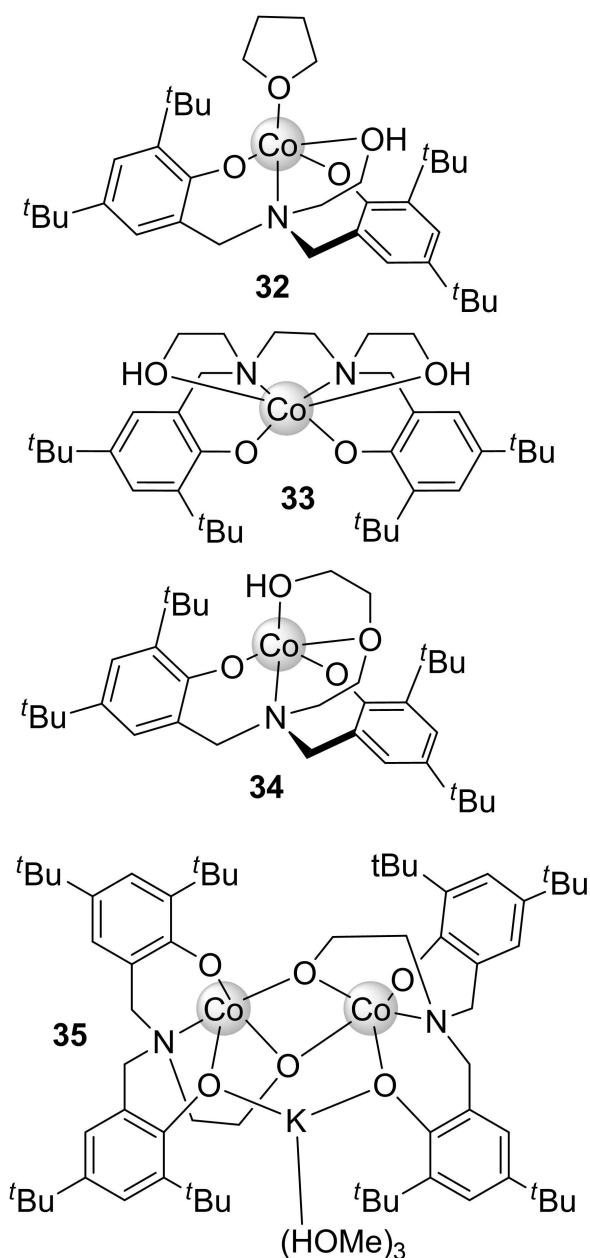


Figure 9. Structures amino-bridged bis(phenolato) Co(II) complexes 32–35.

of Co(II) by air. In the presence of TBAI all these complexes are active in the cycloaddition of CO<sub>2</sub> to ECH (0.1 MPa; 45–75 °C, 24 h). The catalyst **34** is the most active reaching a conversion of 91%.

## 2.2. Polydentate Nitrogen-ligands

Rojas and Gade reported the synthesis of two aluminum complexes supported by a tetradentate amidinate ligand derived from a naphthalene-1,8-bisamidine precursor. The authors reported that the methyl derivative **36** forms the corresponding iodine compound **37** by reaction with I<sub>2</sub> (Figure 10).<sup>[53]</sup> Both compounds are efficient catalysts for the

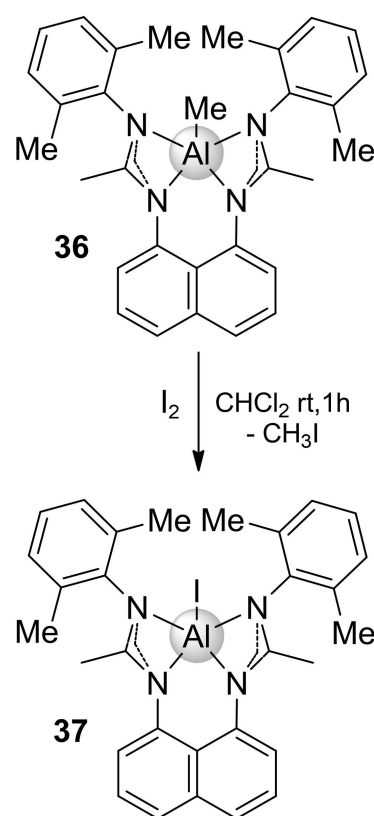


Figure 10. Structures tetradentate amidinate aluminum complexes **36** and **37**.

conversion of various terminal epoxides (0.1 MPa; 80 °C, 24 h) to the corresponding COCs in high yield (up to 93% in the case of SO) but only compound **37** acts as single component catalyst not requiring the presence of an equivalent of onium salt (TBAI) as cocatalyst. Notably **37** is one of the rare examples of non-zwitterionic single component catalysts.

Fe(II) iminopyridine complexes **38–42** promote the conversion of SO to the corresponding carbonate as single component catalysts (0.5 MPa; 80 °C, 20 h) with a maximum conversion of 95% in the case of the catalyst **38** (Figure 11).<sup>[54]</sup> In this case a catalyst loading of 0.5% was necessary in order to reach good catalytic activity. A reduction of catalyst loading to 0.1% was possible activating complex **42** with 10 equivalents of 1,5,7-triazabicyclo[4.4.0]dec-5-ene hydroiodic acid (TBD-HI). In this case, SO is converted to SC (4 MPa; 120 °C, 20 h) with a TOF up to 1609 h<sup>-1</sup>.<sup>[55]</sup>

These systems are also able to convert internal epoxides and to form oxazolodinones from aziridines using tetra-phenyl-phosphonium iodide (TPPI) as cocatalyst.

## 2.3. Macrocyclic ligands

Macrocyclic ligands such as porphyrin and related ligands have been widely used as platform to support various metals in CO<sub>2</sub>/epoxide chemistry.<sup>[56]</sup>



- 38)**  $R_1 = R_2 = \text{CH}(\text{CH}_2\text{OH})_2$   
**39)**  $R_1 = R_2 = (\text{CH}_2)_3\text{OH}$   
**40)**  $R_1 = R_2 = (\text{CH}_2)_3\text{Imid}$   
**41)**  $R_1 = (\text{CH}_2)_3\text{OH}; R_2 = (\text{CH}_2)_3\text{Imid}$   
**42)**  $R_1 = (\text{CH}_2)_3\text{Imid}; R_2 = (\text{CH}_2)_3\text{OH}$

Figure 11. Structures of Fe(II) iminopyridine complexes 38–42.

Recently, Milani and coworkers reported the behavior of various porphyrazines complexes bearing bivalent metal ions [Mg(II), Zn(II), Co(II), Cu(II)] (43–48, Figure 12).<sup>[57]</sup> The initial screening shows a superior performance, with PO (3 MPa; 140 °C, 3 h), of the magnesium catalysts *vis-à-vis* the other metal centers with the highest TOF of 12893 h<sup>-1</sup> observed for the complex 43 bearing the electron withdrawing –CF<sub>3</sub> groups.

It is worth noting that this system, however, requires a large excess of cocatalyst (40 eq.) to assure high activity. Furthermore, the authors also showed that, in the presence of a large excess of cocatalyst, the halide ion can coordinate to the metal center, acting as poison, with the formation of an inactive species and consequently lowering the catalytic activity. This tendency is more pronounced for the Cl<sup>-</sup> ion, decreases for Br<sup>-</sup> and

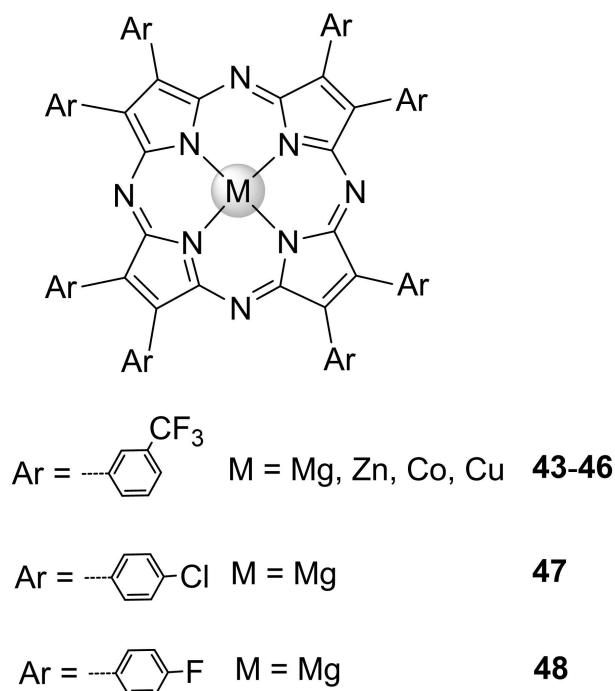


Figure 12. Structures of porphyrazines complexes 43–48.

negligible the case of I<sup>-</sup> with the consequence that the order of activity depends on the choice of the cocatalyst with the following order: TBAI > TBAB ≫ TBAC.

Following previous works on metallate single-component catalysts,<sup>[43,47]</sup> a catalyst based on a ferrate ion supported by a pyridine-containing macrocyclic ligand was reported by Caselli and coworkers (49, Figure 13).<sup>[58]</sup>

Indeed, the ferrate complex 49 acts as catalyst for the conversion of SO to SC (0.8 MPa; 125 °C, 3 h) with a TOF up to 132 h<sup>-1</sup>. The system also allows the conversion, although with lower activity, of other terminal epoxides and CHO to the corresponding carbonates.

A cyclic ligand, designed combining the successful example of the Robson-type ligand employed in the CO<sub>2</sub>/epoxide reactions with various metal centers by Williams and coworkers,<sup>[59–62]</sup> with the beneficial role played by the soft sulfur atom in the ligand design for the CO<sub>2</sub>/epoxides coupling,<sup>[63]</sup> was reported by He and coworkers (Figure 14).<sup>[64]</sup> In particular they reported that the bimetallic complexes 50–53 activated by TBAB displayed higher activity (TOF up to 4188 h<sup>-1</sup> for the complex 52) in the conversion of PO to PC compared to the corresponding mononuclear complex 53 (TOF = 1392 h<sup>-1</sup>) under the same reaction conditions (3 MPa; 130 °C, 1 h).

This fact suggests a cooperative mechanism between the two metal centers as depicted in Scheme 4 with one metal center coordinating the epoxide and the other one activating the CO<sub>2</sub> (A) with the nucleophile furnished by the onium salt TBAB or TBAN<sub>3</sub> (B) followed by the ring-closing step (C). The good performances of these macrocyclic complexes were also confirmed with other terminal epoxides and with CHO and vinyl-cyclohexene oxide (VCHO) with the exclusive formation of cyclic product. Notably the catalyst 52 is also high tolerant to common impurities such as O<sub>2</sub>, NH<sub>3</sub>, CO and H<sub>2</sub>O and can be reused seven times without loss of activity.

### 3. Polycarbonates

Direct reaction of CO<sub>2</sub> with epoxides can also lead to the formation of aliphatic polycarbonates (APCs). In the last

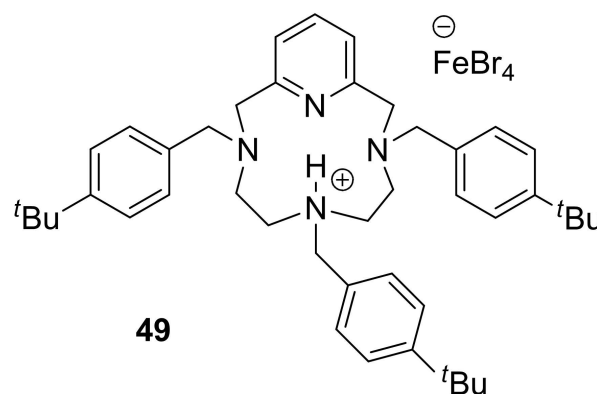


Figure 13. Structures of pyridine-containing macrocyclic ligand-based complex 49.

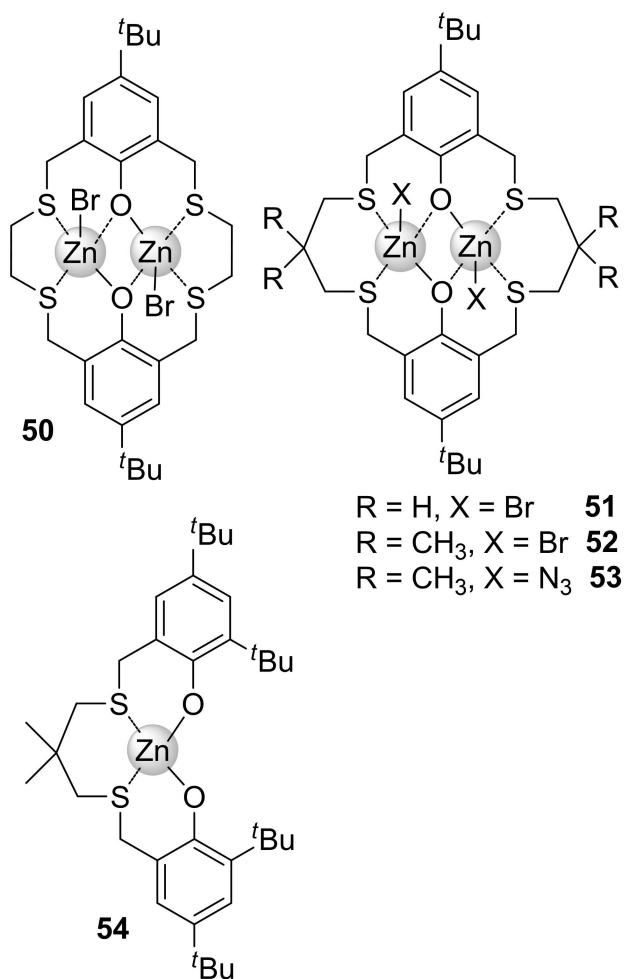
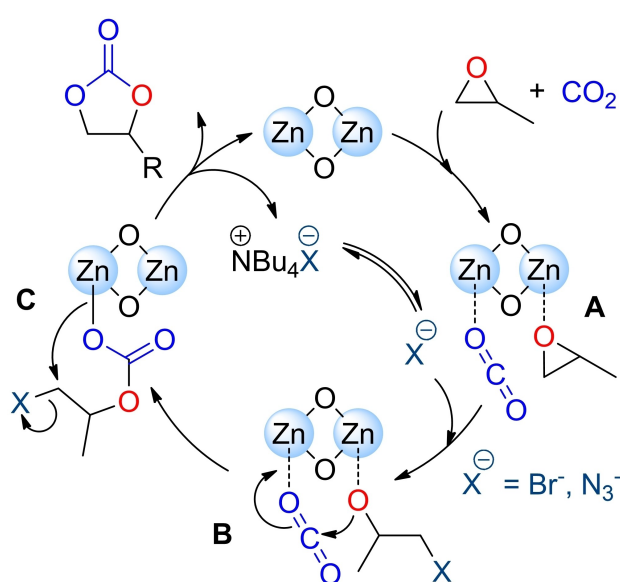


Figure 14. Structures of macrocyclic thioether-phenoxy ligand-based complexes 50–54.



Scheme 4. Proposed reaction mechanism for the formation of cyclic carbonates catalyzed by complexes 50–54.

decades, APCs gained much attention due to raising concern regarding the use and *end-of-life* disposal of well-assessed aromatic polycarbonates. Indeed, APCs demonstrated to be generally biocompatible and biodegradable rendering these polymers good candidates as more sustainable materials. Numerous catalytic systems have been proposed for this transformation, with the most efficient being often based on metals such as Co and Cr. However, the synthesis of APCs via CO<sub>2</sub>/epoxides ring-opening copolymerization (ROCOP) remains an attractive research topic and several challenges are still open, such as:

- the search for very high-performance catalysts based on more-benign metals (e.g., Zn, Mg, Fe, and Al);
- the design of catalytic systems capable to polymerize structurally diverse epoxides (in most cases only CHO can be used);
- profound comprehension of reaction mechanism and factors governing chemo- and stereo-selectivity.

Here we summarize the major advancement achieved in these respects during the last few years, dividing the results on the bases of the ligand structure.

### 3.1. Salen and salen-like ligands

In 2018, Williams et al. reported the first indium-based catalyst for the ROCOP of CO<sub>2</sub> and CHO, based on phosphasalén ligands (complexes 55–61, Figure 15).<sup>[65]</sup>

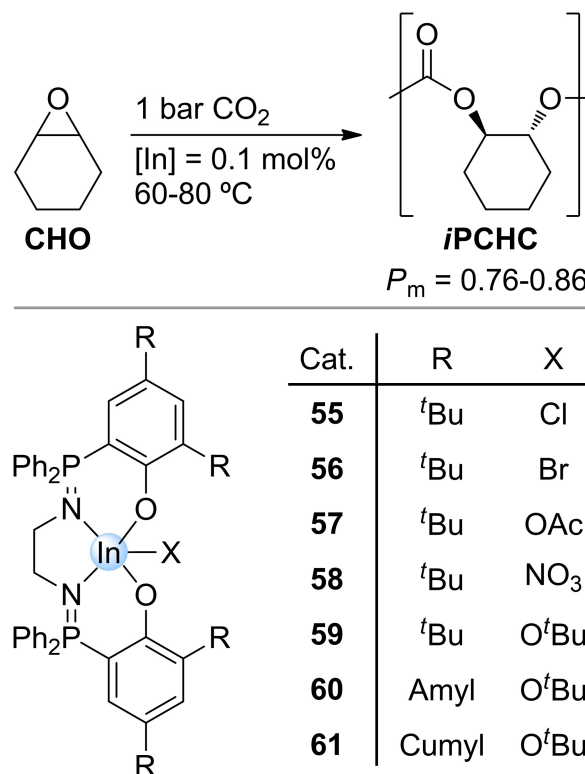
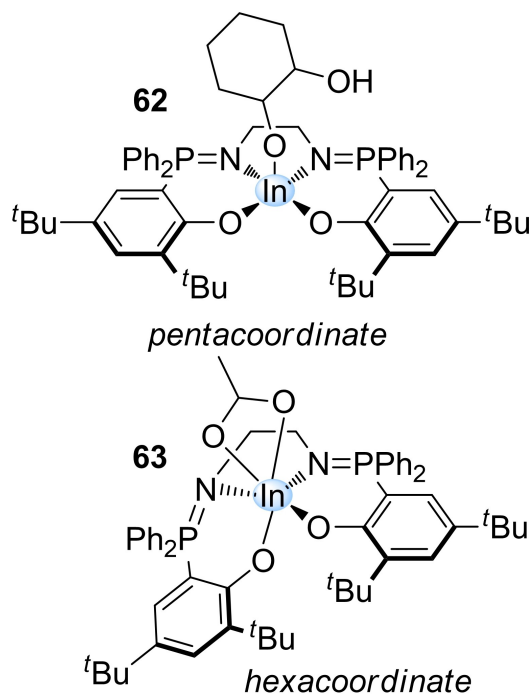
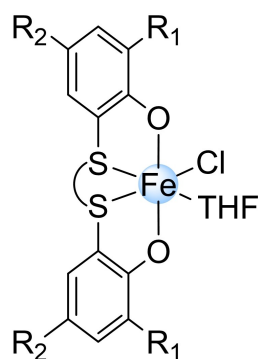


Figure 15. Indium phosphasalén complexes 55–61 studied for isotactic poly(cyclohexene carbonate) iPCHC synthesis.

Notably, these catalysts allowed for the synthesis of isotactic poly(cyclohexene carbonate) (*i*PCHC) under low CO<sub>2</sub> pressure (i.e., 1 bar), without the use of cocatalyst. In particular, the bulkier complex **61** resulted the more efficient (TOF = 15 h<sup>-1</sup>) giving *i*PCHC with the highest stereoselectivity (*meso* triad probability, *P<sub>m</sub>*, of 0.86).



**Figure 16.** Structures of model catalytic intermediates Indium phosphasalen complexes **62** and **63**.



Cat.	( )	R <sub>1</sub>	R <sub>2</sub>
<b>64</b>	(CH <sub>2</sub> ) <sub>2</sub>	Trityl	Me
<b>65</b>	(CH <sub>2</sub> ) <sub>2</sub>	Cumyl	Cumyl
<b>66</b>	(CH <sub>2</sub> ) <sub>2</sub>	Me	Me
<b>67</b>	<i>c</i> -Hex	<i>t</i> Bu	<i>t</i> Bu

**Figure 17.** Iron [OSSO]-type complexes **64–67**.

A mechanistic investigation was conducted based on kinetic experiments, revealing a first order in catalyst concentration and zero-order in carbon dioxide pressure. Unfortunately, reaction order with respect to CHO was not determined due to the exclusive formation of CHC after dilution with diethylcarbonate. The isolation of two model complexes, resembling intermediate species in the catalytic cycle, was achieved (**62** and **63**, Figure 16). The X-ray structural analyses revealed that indium is pentacoordinate in the alcoholate species **62**, while in the case of acetate species **63** indium is hexacoordinate. Based on these observations, a monometallic copolymerization mechanism was proposed.

Recently, the mechanism of CO<sub>2</sub>/CHO ROCOP catalyzed by In-phosphasalen complexes was investigated using DFT methods.<sup>[66]</sup> The authors propose that the rate-determining ring-opening step of In-coordinated CHO occurs via a monometallic transition state, involving the intermolecular attack by a dissociated carbonate species. In addition, isotacticity levels predicted in this study were in good agreement with the experimental ones.

In parallel with the group of Williams, we and others reported on the use of new iron complexes based on [OSSO]-type ligands for the reaction of CO<sub>2</sub> with several terminal and internal epoxides (complexes **64–67**, Figure 17).<sup>[43]</sup> These [OSSO]-Fe complexes, in combination with a halide cocatalyst, resulted in a highly active catalytic system for the preparation of COCs from a series of terminal and internal oxiranes at low temperature and CO<sub>2</sub> pressure (namely 35 °C and 1 bar). However, the same system converts CHO and CO<sub>2</sub> in PCHC with virtually perfect selectivity, with a TOF up to 400 h<sup>-1</sup>. Numeral average molecular weights (*M<sub>n</sub>*) varied in the range from 4 to 28 kDa. Differently from the indium phosphasalen system, atactic polycarbonates were obtained. Notably, complex **65** was also active without any cocatalyst (TOF = 27 h<sup>-1</sup>), however a low content of carbonate linkages was obtained in the final polymer.

A combined kinetic and computational mechanistic investigation was performed revealing that the copolymerization process follows a monometallic reaction pathway with the CHO insertion onto the growing polymer chain being the rate determining step.

Later, dinuclear iron complexes based on a tailored multi-dentate bis-[OSSO] ligand were reported from the same group obtaining similar results in propylene carbonate and PCHC formation supporting different bimetallic-monometallic mechanisms.<sup>[44,63]</sup> The results obtained with [OSSO]-Fe systems triggered the interest for studying structurally related complexes based on different metals. At this purpose, the catalytic behavior of [OSSO]-chromium complexes (**68–72**, Figure 18) was investigated.<sup>[68,69]</sup>

At first, the ROCOP of CO<sub>2</sub> with several epoxides was studied using complex **68** activated with PPNCl (Figure 19). As for the [OSSO]-Fe complexes, PCHC was obtained with full selectivity but with lower activity (TOF = 19 h<sup>-1</sup>). Differently it was found that, in the case of terminal epoxides such as propylene oxide, the COC/PC selectivity depends on reaction temperature reaching more than 90% PC selectivity at 45 °C. Notably, polystyrene

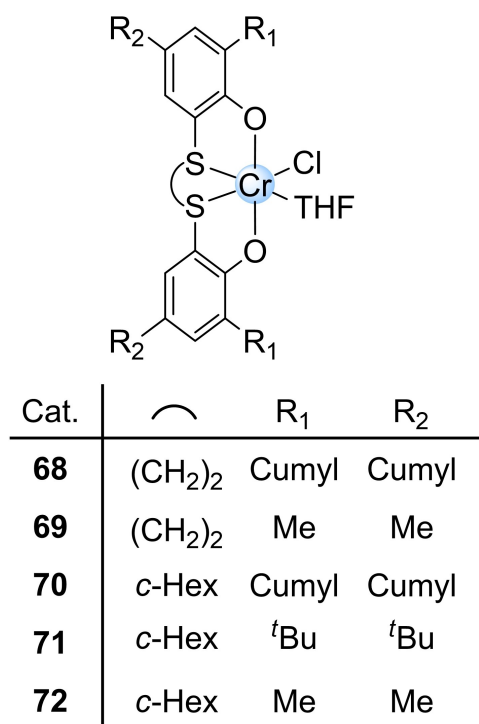


Figure 18. Chromium [OSSO]-type complexes 68–72, studied for polycarbonates synthesis.

carbonate was also obtained even with low polymer selectivity (32%). Using the same catalytic system, it was possible to conduct terpolymerization reactions starting from a mixture of propylene oxide with 1,2-hexene oxide or cyclohexene oxide obtaining random PPC-*co*-PHC or blocky PPC-*b*-PCHC respectively.

Following this initial study, the effect of ligand structure on the ROCOP was explored and it was found that the presence of bulky substituents on the phenol rings is crucial to obtain good catalytic activity and polycarbonate selectivity. For example, at 45 °C and 20 bar CO<sub>2</sub> pressure, complex 68 produces poly(propylene carbonate) (PPC) with 93% selectivity and a TOF of 35 h<sup>-1</sup> while the less hindered complex 69 produces only propylene carbonate with a TOF of 7 h<sup>-1</sup>.

In 2020, Kirillov described the synthesis and characterization of a series of mono- and dinuclear rare-earth metals complexes supported by polydentate bis(imino)phenoxy and bis(amino)phenoxy ligands.<sup>[70]</sup>

In this study, the authors reported that one mononuclear yttrium complex (73, Figure 20) is active in the copolymerization of CO<sub>2</sub> with CHO. Good activity was observed at relatively mild conditions (70 °C, 12 bar), however PCHC with *M<sub>n</sub>* < 12 kDa and 1.5 < *D* < 8.3 was obtained. Interestingly, kinetic investigation also suggest that a monometallic reaction mechanism occurs in this case.

Recently Yao et al. reported the synthesis and characterization of new mono- and dinuclear rare-earth metals com-

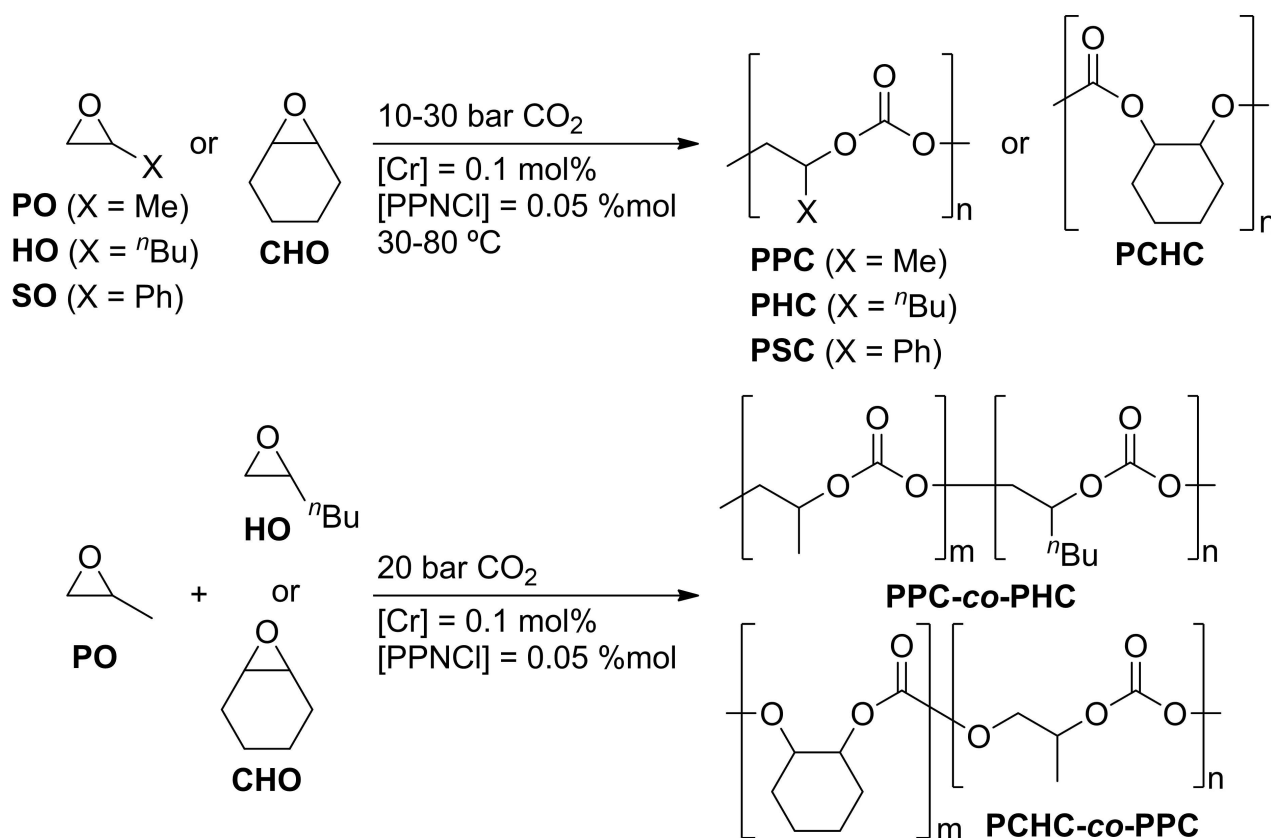
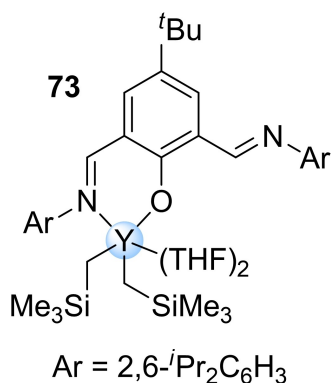


Figure 19. Copolymerization and terpolymerization reactions conducted with chromium [OSSO]-type complex 68.



**Figure 20.** Yttrium bis(imino)phenoxy complex **73** studied for poly(cyclohexene carbonate) synthesis.

plexes supported by *o*-phenylenediamine-bridged triphenolate ligands (Figure 21).<sup>[71]</sup>

In this case benzyl alcohol was used as the initiator and complex **76** resulted the most efficient, converting 335 equivalents of CHO in 18 h at 70 °C and 20 bar CO<sub>2</sub>. Several

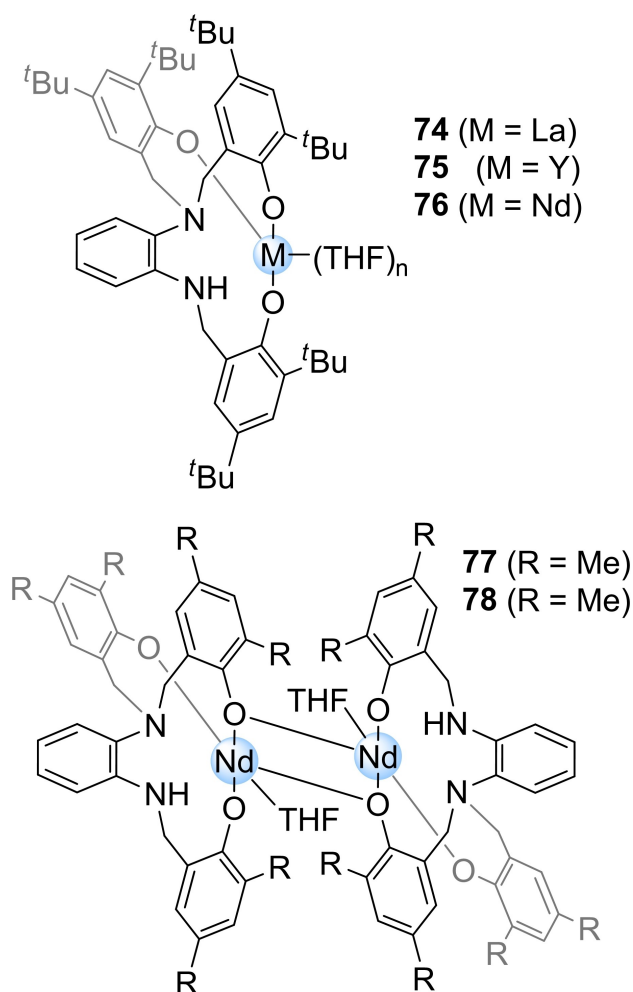


**Figure 21.** Rare-earth *o*-phenylenediamine-bridged triphenolate complexes **74–78** studied for poly(cyclohexene carbonate) synthesis.

solvents were tested for the reaction, but polymers with broad molecular weights distribution were obtained in all cases ( $3.1 < \bar{M}_w < 7.0$ ). The initiation with benzyl alcohol was demonstrated by PCHC MALDI-TOF analysis. In addition, a dinuclear Nd complex coordinated with a benzyl alcohol molecule was isolated from **77** and characterized by X-ray analysis. Such complex showed the same activity observed with the system **77**/BnOH, suggesting that it is in fact formed in situ under the reaction condition.

In 2020, Williams et al. reported the use of titanium-amino-triphenolate complexes for the synthesis of PCHC (**79–83**, Figure 22).<sup>[72]</sup>

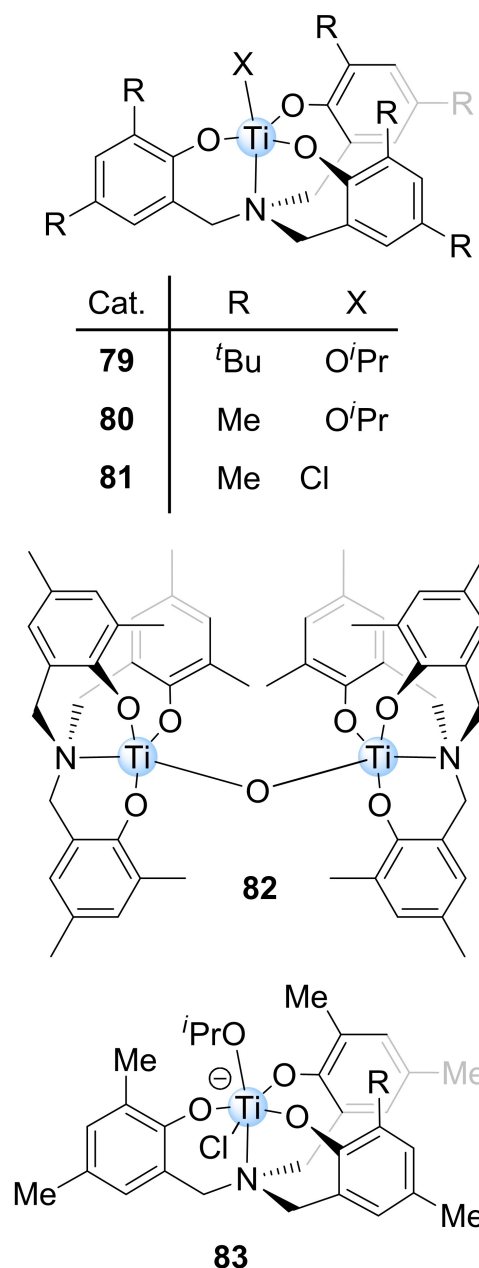


**Figure 22.** Titanium amino triphenolate complexes **79–83** studied for poly(cyclohexene carbonate) synthesis.

In this case, the less hindered alcoholate complex **80** resulted the most efficient, reaching a  $t$  TOF of  $135 \text{ h}^{-1}$  at  $120^\circ\text{C}$ . In addition, a linear increase of molecular weights with conversion was observed indicating a good control of the polymerization process. Interestingly, the anionic hexacoordinate titanium complex **83** was isolated by reaction of complex **80** and  $\text{PPh}_4\text{Cl}$  and characterized by X-ray diffraction analysis. This complex **83** was proposed as model of an intermediate formed during the catalytic cycle and responsible for the initiation of the copolymerization process by ring-opening of cyclohexene oxide to form a titanium-alcoholate species.

### 3.2. Macrocyclic ligands

Porphyrins have been widely used for the production of both COCs and PCs.<sup>[73–77]</sup> Also with these systems the interaction between metal centre and cocatalyst plays a key role in determining the catalytic activity, with notable example dated back to the early 80's.<sup>[78]</sup>

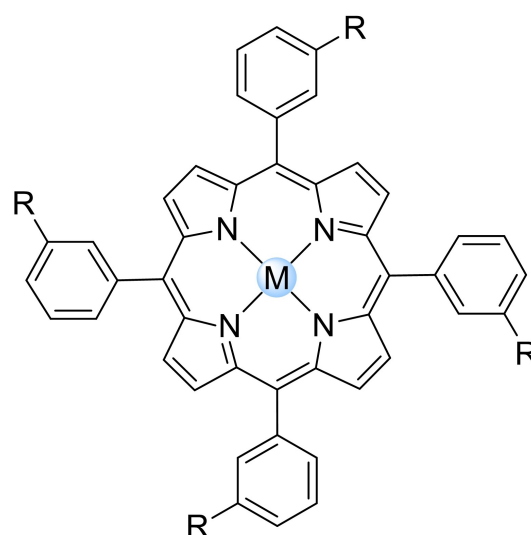
In this frame, Nozaki, Ema et al. described the use of a series of aluminium-, magnesium- and zinc-complexes, based on porphyrin ligands containing ammonium halide moieties connected with flexible alkyl arms (**84–89**, Figure 23).<sup>[79]</sup>

Remarkably, this ligand design allowed for the obtainment of very high catalytic activity, with the aluminum complexes **84** and **85** reaching TOF of  $10000 \text{ h}^{-1}$  at  $120^\circ\text{C}$  and 20 bar of  $\text{CO}_2$ . Also important, PCHC with high  $M_n$  of 281 kDa was obtained using a low catalyst loading of 0.001%. Mechanistic investigation was performed combining kinetic experiments and DFT calculations to understand the origin of this performances. The authors proposed that the presence of quaternary ammonium groups on the catalyst structure prevent the diffusion of anionic growing polymer chain with inhibition of the back-biting process. This in turn reflect on high selectivity at high temperature and allows the obtainment of high molecular weights.

Among all the catalytic systems reported for  $\text{CO}_2/\text{CHO}$  copolymerization, homodinuclear Co, Fe, Zn and Mg complexes based on a "reduced Robson's ligand" have been widely studied by the research group of Williams during the last fifteen years, and this topic has been extensively reviewed.<sup>[80,81]</sup> However, in the last years very interesting results have been obtained using heterodinuclear complexes supported by the same ligand and other macrocyclic ligands.

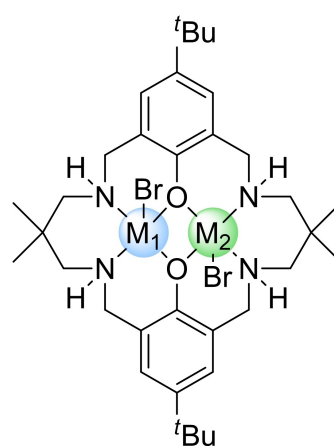
In 2015, the use of heterodinuclear Mg–Zn complex **90** (Figure 24) was reported for the ROCOP of CHO with  $\text{CO}_2$ .<sup>[82]</sup>

Notably, tested under the same conditions (i.e., 0.1 mol% of catalyst,  $80^\circ\text{C}$ , 1 bar), Mg–Zn heterobimetallic complex **90** exhibits a higher activity ( $\text{TOF} = 34 \text{ h}^{-1}$ ) when compared with its homodinuclear Mg- (**92**,  $\text{TOF} = 15 \text{ h}^{-1}$ ), and Zn- (**91**, inactive) analogues. A similar effect was observed in the related ROCOP of CHO with phthalic anhydride to obtain the corresponding polyester. In the attempt to explain this behavior, it was proposed that the positive synergic effect is due to the combination of two effects: on one hand the Lewis acid Zn-center activates the epoxide, on the other the Mg-center



Cat.	M	R
<b>84</b>	AlCl	$\text{O}(\text{CH}_2)_6\text{N}^+(\text{}^n\text{Bu})_3\text{Cl}^-$
<b>85</b>	AlBr	$\text{O}(\text{CH}_2)_6\text{N}^+(\text{}^n\text{Bu})_3\text{Br}^-$
<b>86</b>	Mg	$\text{O}(\text{CH}_2)_6\text{N}^+(\text{}^n\text{Bu})_3\text{Cl}^-$
<b>87</b>	Mg	$\text{O}(\text{CH}_2)_6\text{N}^+(\text{}^n\text{Bu})_3\text{Br}^-$
<b>88</b>	Zn	$\text{O}(\text{CH}_2)_6\text{N}^+(\text{}^n\text{Bu})_3\text{Cl}^-$
<b>89</b>	Zn	$\text{O}(\text{CH}_2)_6\text{N}^+(\text{}^n\text{Bu})_3\text{Br}^-$

Figure 23. Porphyrin complexes **84–89** bearing ammonium halide pendant moieties.



Cat.	M <sub>1</sub>	M <sub>2</sub>
<b>90</b>	Zn	Mg
<b>91</b>	Zn	Zn
<b>92</b>	Mg	Mg

Figure 24. Structure of heterodinuclear Zn–Mg complex **90** and homodinuclear complexes **91** and **92**.

enhances the carbonate attack on for the ring-opening step of the oxirane ring.

On the bases of these results, other heteronuclear Zn-based complexes supported by the same macrocyclic ligand were

prepared and investigated in ROCOP reactions. First, the use of heterobimetallic Zn–Ti complexes **93** and **94** was studied (Figure 25).<sup>[83]</sup> The selective installation of a single Ti(IV)-center prior to the formation of the final complexes allowed the simple preparation of catalysts **93** and **94**. However, only modest

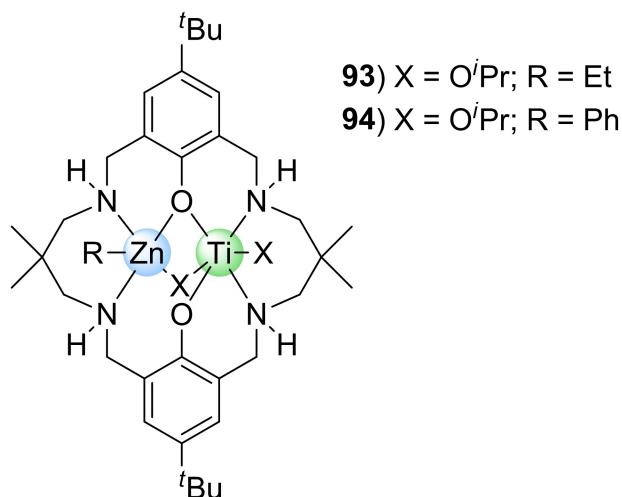
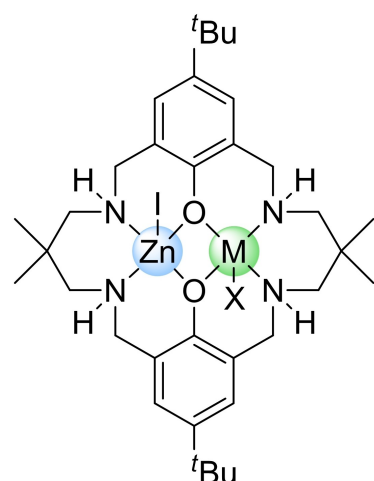


Figure 25. Heterodinuclear Zn–Ti-complexes **93** and **94**.



Cat.	M	X
<b>95</b>	Li	I
<b>96</b>	Li	OBzpCF <sub>3</sub>
<b>97</b>	Na	I
<b>98</b>	K	I
<b>99</b>	K	OBzpCF <sub>3</sub>
<b>100</b>	Mg	I
<b>101</b>	Ca	I

Figure 26. Heterodinuclear Zn–Group 1,2-complexes **95**–**101**.

activity was recorded with a TOF of 3 h<sup>-1</sup> in the case of **94**. In addition, molecular weights lower than 2.2 kDa were obtained.

Later, heterodinuclear complexes based on Zn and Group 1 and 2 metals were tested in the CHO/CO<sub>2</sub> copolymerization (complexes **95**–**101**, Figure 26).<sup>[84]</sup>

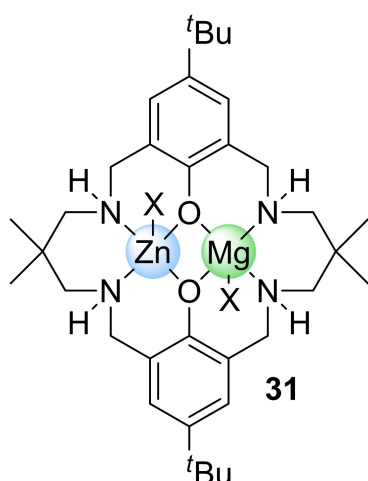
Interestingly, iodide Li-, K-, and Ca-based complexes **95**, **98** and **101** only produced *cis*-CHC while Li-, and K-based complexes **96** and **99**, with a *p*-trifluoromethyl-benzoate (OBzpCF<sub>3</sub>) ligand, produced PCHC with high selectivity and small amounts of *trans*-CHC. However, all these complexes were less active than the homonuclear Zn complex. On the contrary, Mg-complex produced PCHC with high activity (TOF = 72 h<sup>-1</sup>) and selectivity (99%). This difference was ascribed to the competition between back-biting reaction on I-opened carbonate, forming *cis*-CHC, and CHO insertion in the metal-carbonate bond, forming PCHC.

Finally, Zn–Mg heterobimetallic complexes with different monoanionic acetate or benzoate ligands were prepared and studied in the ROCOP reaction (**102**–**110**, Figure 27).<sup>[85]</sup>

Under relatively mild conditions (i.e., 0.1 mol% of catalyst, 80 °C, 1 bar) all the complexes were more active than the homometallic congener, and good activities recorded with TOF values varying from 43 h<sup>-1</sup> for **104**, to 124 h<sup>-1</sup> for **108**. The resulting PCHC has the bimodal molecular weight distribution typical of this process, with *M<sub>n</sub>* from 3.0 to 19 kDa. Notably, PCPC with *M<sub>n</sub>* up to 42 kDa was also obtained with high selectivity using complex **106**. High activity was recorded using complex **107**, reaching a TOF of 8830 h<sup>-1</sup> at higher temperature and pressure (120 °C, 20 bar), but lower catalyst loading (0.01 mol%).

Kinetic investigations were conducted using complex **109**. A first order dependance was observed for both catalyst and CHO concentration, while a zero order dependance was obtained for carbon dioxide. Consequently, the CHO ring-opening was pointed as the rate determining step (*rd*s). However, to understand which metal center coordinates the epoxide and which one binds the carbonate-ended polymer chain, DFT investigations were performed, and it was found that the reaction pathway through the Mg-coordinated CHO has a lower activation barrier for the *rd*s. In addition, the crystal structure of the related complex **100**, obtained from THF, shows that the solvent molecule is coordinated to the Mg-center. Based on these results, it was proposed that the actual *rd*s presents the CHO monomer coordinated to the Lewis acid Mg-center, while the Zn-center promotes the attack by the carbonate group of the growing-polymer chain (Figure 28).

More recently, heterobimetallic Mg–Co(II) complex **111** was reported to have significantly higher activity with respect to the previously described Zn–Mg system (Figure 29a).<sup>[86]</sup> In fact, a high TOF value of 12460 h<sup>-1</sup> was obtained for the copolymerization of CHO with CO<sub>2</sub> at 140 °C and 20 bar. A detailed kinetic investigation supported a scenario similar to that of Zn–Mg system, with the Mg-center coordinating CHO and the Co-center promoting the attack of the polymer chain on the epoxide (Figure 29b). In addition, comparing the results obtained with homonuclear Co–Co and Mg–Mg complexes, it was possible to understand the origin of the relatively low Δ*G*<sup>‡</sup>



Cat.	X	R
102	Br	
103	OAc	
104		
105		H
106		OMe
107		CF <sub>3</sub>
108		NO <sub>2</sub>
109		NMe <sub>2</sub>
110		F

Figure 27. Structure of heterodinuclear Zn–Mg complex 102–110.

as the combination of two effects. On one hand, magnesium reduces the  $\Delta S^\ddagger$  by strongly coordinating the epoxide; on the other, cobalt reduces the  $\Delta H^\ddagger$  for the ring-opening step by rendering the carbonate moiety more nucleophilic.

All these studies on heterometallic systems allowed a much clearer comprehension of CO<sub>2</sub>/epoxide reaction mechanism and paved the way for following investigations. Indeed, very recently the same research group reported the use of other heterometallic dinuclear and trinuclear catalytic systems based on different macrocyclic ligands.

In 2020, a new heterobimetallic Co(III)/Group 1 metals catalytic system for the copolymerization of CO<sub>2</sub> with PO was developed, supported by a properly designed ligand encompassing a Salen and a crown-ether-like moieties (Figure 30).<sup>[87]</sup>

With this system, the efficient preparation of polypropylene carbonate (PPC) was achieved, reaching TOF of 800 h<sup>-1</sup> in the case of Co/K complex 113. Polycarbonates with  $2.3 \leq M_n \leq$

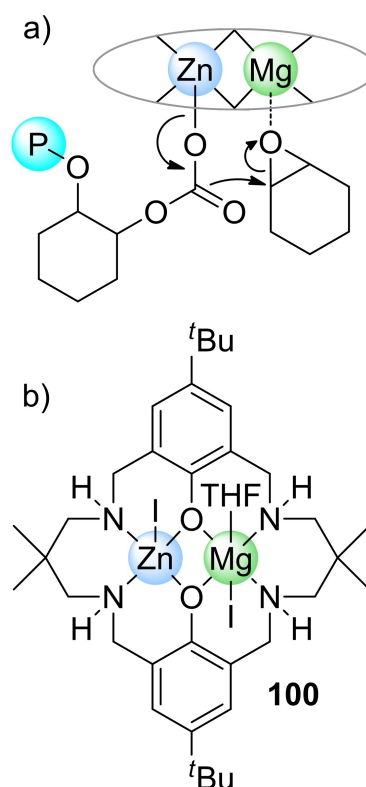
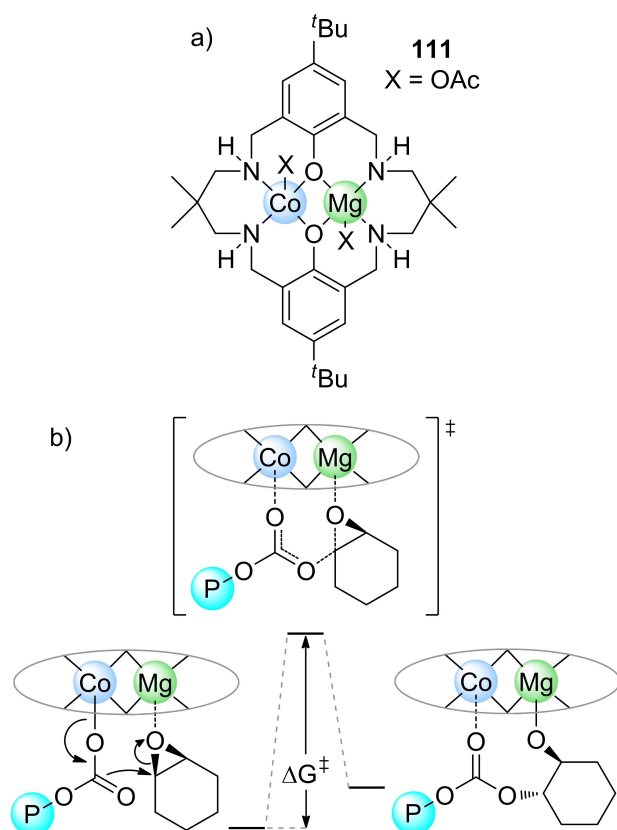


Figure 28. Proposed intermediate for the ring-opening *rds* step with Mg-coordinated CHO for the CHO/CO<sub>2</sub> ROCOP promoted by heterodinuclear Zn–Mg catalyst (a), and complex 100 structure.

8.8 kDa were obtained with narrow polydispersity indexes  $1.04 \leq \mathcal{D} \leq 1.10$  but bimodal MW distributions. Notably, catalyst 113 can be employed at low catalyst loading (0.01 mol%) in combination of 1,2-cyclohexanediol as chain-transfer agent (CTA) reaching good control on MW's. For example, monomodal PPC polyol with  $M_n = 7.0$  kDa and  $\mathcal{D} = 1.07$  was obtained using 100 equivalents of CTA with respect to the catalyst. Remarkably, the ROCOP of CO<sub>2</sub> with other terminal epoxides, such as vinyl-oxirane, allyl glycidyl ether, tert-butyl glycidyl ether, and internal epoxides, such as cyclohexene oxide, vinyl cyclohexene oxide and cyclopentene oxide, was also achieved.

Following this first repost, structurally different heterobimetallic complexes based on Na in combination with Zn, Mg and Co were studied in the copolymerization of CHO with CO<sub>2</sub> in order to get insights into the structure-activity relationship of these new catalysts (complexes 116–123, Figure 31).<sup>[88]</sup>

From the comparison of catalytic activities of complexes 116–123 and the previously reported complex 112 it was found that the rigidity of the backbone from 2,2-dimethylpropane-bridge to ethyl-bridge ligand resulted in an enhancement of catalytic activity (e.g., 118 exhibits a TOF of 581 h<sup>-1</sup> while 112 shows a TOF of 759 h<sup>-1</sup>). Nevertheless, a further increase of rigidity by introduction of 1,2-benzene-bridge has a detrimental effect on TOF (i.e., complex 123 exhibits a TOF of 176 h<sup>-1</sup>). In summary, the heterobimetallic Co–Na catalyst 112 resulted the most efficient of the series.



**Figure 29.** Structure of heterodinuclear Co–Mg complex **111** (a), and rate determining step for the ROCOP of CHO with CO<sub>2</sub> (b).

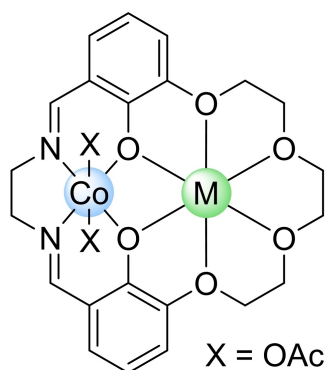
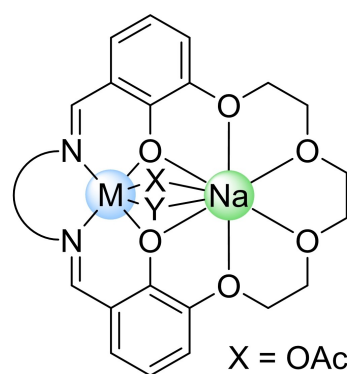


**Figure 30.** Structure of heterodinuclear Co–Group 1 metals complexes **112**–**115**.

In 2021, a new heterotrimetallic Zn<sub>2</sub>Na complex was reported as switchable catalyst in ROCOP reactions (**124**, Figure 32a).<sup>[89]</sup> In this case, zinc and sodium were judiciously combined with the intent to introduce poly(cyclohexene oxide) (PCHO) polyether linkages into the PCHC, with the aim to increase polycarbonate stability toward depolymerization phenomena under industrial conditions. Complex **124** produces PCHC with high selectivity and activity (TOF = 2900 h<sup>-1</sup>) under high temperature and pressure (120 °C, 20 bar). However, when CO<sub>2</sub> pressure is reduced, polyether linkages are incorporated into the polymer chain yielding the desired PCHC-*ran*-PCHO



Cat.	M	Y
<b>116</b>	Zn	-
<b>117</b>	Mg	-
<b>118</b>	Co(III)	OAc
<b>119</b>	Zn	-
<b>120</b>	Mg	-
<b>121</b>	Zn	-
<b>122</b>	Mg	-
<b>123</b>	Co(III)	OAc

**Figure 31.** Structure of heterodinuclear Na–Zn, Na–Mg and Na–Co complexes **116**–**123**.

(Figure 32b). For example, at 1 bar of CO<sub>2</sub> and 120 °C, 33% of polyether is incorporated into the final polymer. Notably, the catalyst remains active at CO<sub>2</sub> pressure lower than 1 bar. Indeed, using a mixture of 0.5 bar CO<sub>2</sub> and 0.5 bar N<sub>2</sub> at 80 °C, a copolymer with polycarbonate/polyether ratio equal to 41/59 was obtained with a TOF = 200 h<sup>-1</sup>. The authors also explored the possibility to use complex **124** as switchable catalyst combining the ROCOP of CHO with phthalic anhydride (PA) and CHO/CO<sub>2</sub> copolymerization. Highly remarkably, they succeeded in the preparation of multiblock copolymers like the P(CHO-*alt*-PA)-*b*-PCHC-*b*-PCHO (Figure 32b) by starting the reaction in the presence of PA and excess of CHO, followed by introduction of CO<sub>2</sub> at the desired reaction time.

Later, various heterotrimetallic complexes were prepared to study the relationship between catalyst-structure and activity (complexes **125**–**132**, Figure 33).<sup>[90]</sup> First, zinc was replaced with other metals such as Mg, Al, and Co(III), but all the resulting complexes showed activity lower than the native Zn<sub>2</sub>Na complex **124**, or even decomposed like the Al<sub>2</sub>Na complex **126**. Then, the imine-linkers were modified keeping the Zn<sub>2</sub>Na combination. In this case, a significant enhancement in catalytic activity was achieved in the case of complex **132**, bearing the

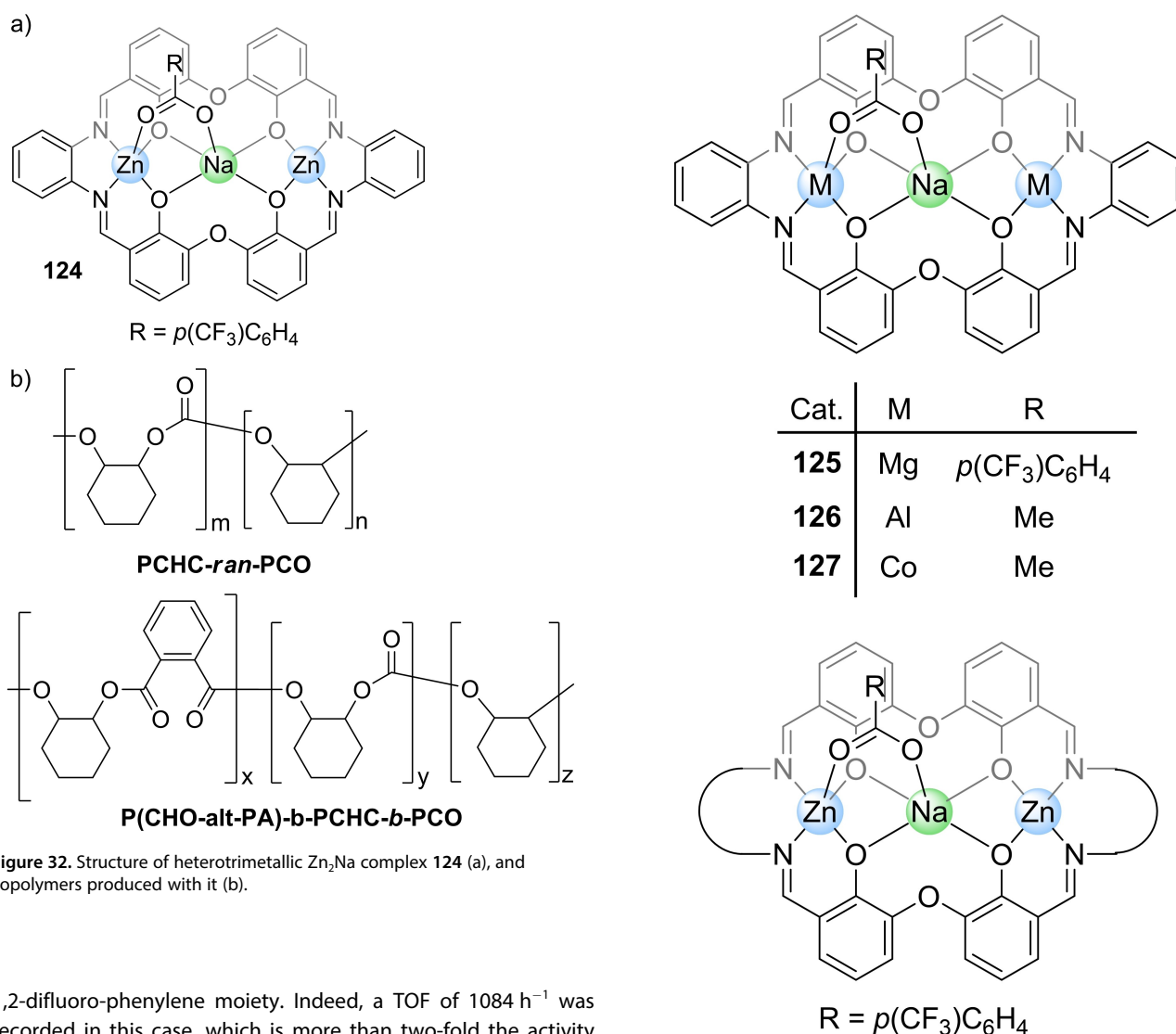


**Figure 32.** Structure of heterotrimeric  $\text{Zn}_2\text{Na}$  complex **124** (a), and copolymers produced with it (b).

1,2-difluoro-phenylene moiety. Indeed, a TOF of  $1084 \text{ h}^{-1}$  was recorded in this case, which is more than two-fold the activity obtained with complex **124** ( $\text{TOF} = 478 \text{ h}^{-1}$ ) under the same conditions (cat. =  $0.025 \text{ mol}\%$ ,  $100^\circ\text{C}$ ,  $1 \text{ bar CO}_2$ ).

In 2019, Love, Williams et al. reported the study of the reaction between tetranuclear Zn-complex **133** with alcohols (Figure 34).<sup>[91]</sup>

In this study, they found that complex **133** and **135**, activated with an alcohol such as n-hexanol, produce PCHC. Under the best conditions reported,  $80^\circ\text{C}$  and  $30 \text{ bar}$  of  $\text{CO}_2$ , PCHC was obtained with 90% content of carbonate linkages and a TOF of  $15 \text{ h}^{-1}$ . However, a very broad distribution of molecular weights was observed ( $M_n = 12 \text{ kDa}$ ;  $D = 14$ ). This was attributed to scarce control in the presence of multinuclear complex subject to demetallation such as in complex **133**.

## 4. Conclusions

In spite of the fact that the reaction between carbon dioxide and epoxides has been intensively studied in the last two decades, the search for more active and selective catalysts remains a major challenge in the field. In particular the use of Earth-crust abundant, less toxic metals showing performances

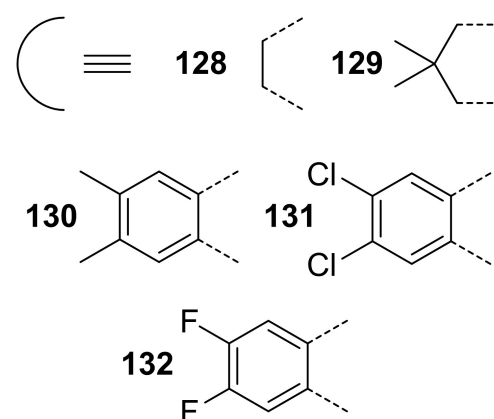


**Figure 33.** Structure of heterodinuclear Na–Zn, Na–Mg and Na–Co complexes **124–132**.

comparable or, in some case superior, to more toxic and high-cost metals is one of the most important issues. Another important point is avoiding the need of using superstoichiometric amount of an onium salt, in combination with the metal

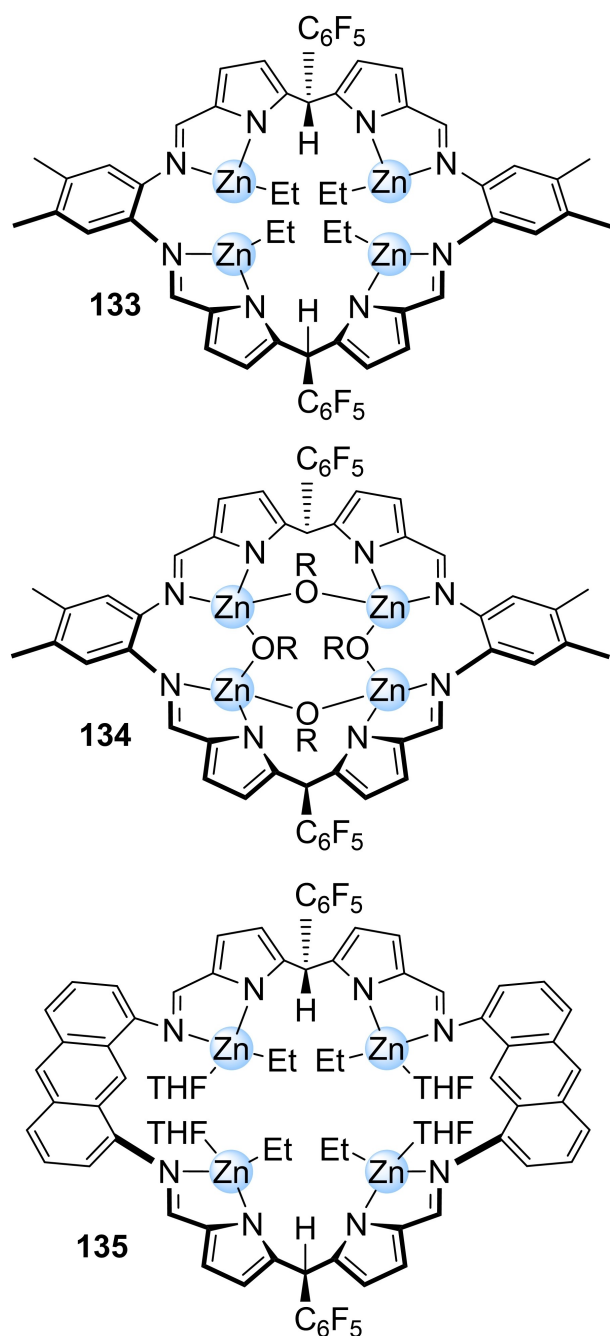


Figure 34. Structure of tetranuclear Zn-complexes 133–135.

complex, to reach high activity by designing single-component catalysts.

Finally, dinuclear and multinuclear catalysts show, especially in the case of the synthesis of polycarbonates, clear advantages in terms of substrate scope, activity and selectivity highlighting the synergic effect of two metal centers in the formation of the polycarbonate chain.

It is worth noting that these trends are not only focused on the obtaining of more reactive and versatile catalysts but also in rendering the reaction between CO<sub>2</sub> and epoxides even more sustainable and in line with the green chemistry principles.

## Acknowledgements

F.D.M. thanks the Università degli Studi dell'Insubria for financial support. C.C. thanks the Università degli Studi di Salerno for financial support. Open Access funding provided by Università degli Studi di Salerno within the CRUI-CARE Agreement.

## Conflict of Interest

The authors declare no conflict of interest.

**Keywords:** Carbon dioxide · Epoxide · Cyclic organic carbonate · Polycarbonate · Catalysis

- [1] C. Hepburn, E. Adlen, J. Beddington, E. A. Carter, S. Fuss, N. MacDowell, J. C. Minx, P. Smith, C. K. Williams, *Nature* **2019**, *575*, 87–97.
- [2] S. Volker, *Faraday Discuss.* **2021**, *230*, 9–29.
- [3] M. M. F. Hassam, L. M. Rossi, D. P. Debecker, K. C. Leonard, Z. Li, B. C. E. Makhubela, C. Zhao, A. Kleij, *ACS Sustainable Chem. Eng.* **2021**, *9*, 12427–12430.
- [4] F. Della Monica, C. Capacchione, in: *CO<sub>2</sub> as a Building Block in Organic Synthesis*, Ed. S. Das, Wiley, 1<sup>st</sup> edn, **2020**, pp. 331–365.
- [5] N. A. Raju, D. Prasad, P. M. Srinivasappa, A. V. Biradar, S. Suryabhan Gholap, A. K. Samal, B. Mallanna Nagaraja, A. H. Jadhav, *Sustain. Energy Fuels* **2022**, *6*, 1198–1248.
- [6] V. Aomchad, A. Cristòfol, F. Della Monica, B. Limburg, V. D'Elia, A. W. Kleij, *Green Chem.* **2021**, *23*, 1077–1113.
- [7] G. A. Bhat, M. Luo, D. J. Darensbourg, *Green Chem.* **2020**, *22*, 7707–7724.
- [8] S. J. Poland, D. J. Darensbourg, *Green Chem.* **2017**, *19*, 4990–5011.
- [9] J. Huang, J. C. Worch, A. P. Dove, O. Coulembier, *ChemSusChem* **2020**, *13*, 469–487.
- [10] V. Paradiso, V. Capaccio, D. H. Lamparelli, C. Capacchione, *Catalysts* **2020**, *10*, 825.
- [11] A. A. Marciniak, K. J. Lamb, L. P. Ozorio, C. J. A. Mota, M. North, *Curr. Opin. Green Sustain. Chem.* **2020**, *26*, 100365.
- [12] F. Della Monica, A. Buonerba, C. Capacchione, *Adv. Synth. Catal.* **2019**, *361*, 265–282.
- [13] R. R. Shaikh, S. Pornpraprom, V. D'Elia, *ACS Catal.* **2018**, *8*, 419–450.
- [14] C. Martin, G. Fiorani, A. W. Kleij, *ACS Catal.* **2015**, *5*, 1353–1370.
- [15] G. Li, S. Dong, P. Fu, Q. Yue, Y. Zhou, J. Wang, *Green Chem.* **2022**, *24*, 3433–3460.
- [16] L. Guo, K. J. Lamb, M. North, *Green Chem.* **2021**, *23*, 77–118.
- [17] G. Fiorani, W. Guo, A. W. Kleij, *Green Chem.* **2015**, *17*, 1375–1389.
- [18] B. Schäffner, F. Schäffner, S. P. Verevkin, A. Börner, *Chem. Rev.* **2010**, *110*, 4554–4581.
- [19] K. Xu, *Chem. Rev.* **2004**, *104*, 4303–4418.
- [20] a) W. Yu, E. Maynard, V. Chiaradia, M. C. Arno, A. P. Dove, *Chem. Rev.* **2021**, *121*, 10865–10907; b) C. Maquilón, F. Della Monica, B. Limburg, A. W. Kleij, *Adv. Synth. Catal.* **2021**, *363*, 4033–40.
- [21] a) N. Bragato, G. Fiorani, *Curr. Opin. Green Sustain. Chem.* **2021**, *30*, 100479; b) B. Limburg, A. Cristòfol, F. Della Monica, A. W. Kleij, *ChemSusChem* **2020**, *13*, 6056–6065; c) P. P. Pescarmona, *Curr. Opin. Green Sustain. Chem.* **2021**, *29*, 100457.
- [22] F. N. Al-Rowaili, U. Zahid, S. Onaizi, M. Khaled, A. Jamal, E. M. AL-Mutairi, *J. CO<sub>2</sub> Util.* **2021**, *53*, 101715.
- [23] W.-L. Dai, S.-L. Luo, S.-F. Yin, C.-T. Au, *Appl. Catal. A* **2009**, *366*, 2–12.
- [24] Y. Qu, Y. Zhao, D. Li, J. Sun, *Curr. Opin. Green Sustain. Chem.* **2022**, *34*, 100599.
- [25] Z. Li, J. Sun, Q. Xu, J. Yin, *ChemCatChem* **2021**, *13*, 1848–1866.
- [26] M. Alves, B. Grignard, R. Mereau, C. Jerome, T. Tassaing, C. Detrembleur, *Catal. Sci. Technol.* **2017**, *7*, 2651–2684.
- [27] F. Han, H. Li, H. Zhuang, Q. Hou, Q. Yang, B. Zhang, C. Miao, *J. CO<sub>2</sub> Util.* **2021**, *53*, 101742.
- [28] M. Mandal, *J. Organomet. Chem.* **2020**, *907*, 121067.
- [29] A. Decortes, A. M. Castilla, A. W. Kleij, *Angew. Chem. Int. Ed.* **2010**, *49*, 9822–9837; *Angew. Chem.* **2010**, *122*, 10016–10032.

- [30] J. Kiriratnikom, N. Laiwattanapaisarn, K. Vongnam, N. Thavornsin, P. Saeng, S. Kaeothip, A. Euapermkiati, S. Namuangruk, K. Phomphrai, *Inorg. Chem.* **2021**, *60*, 6147–6151.
- [31] D. J. Darensbourg, M. W. Holtcamp, *Macromolecules* **1995**, *28*, 7577–7579.
- [32] M. Super, E. Berluce, C. Costello, E. Beckman, *Macromolecules* **1997**, *30*, 368–372.
- [33] M. Cheng, E. B. Lobkovsky, G. W. Coates, *J. Am. Chem. Soc.* **1998**, *120*, 11018–11019.
- [34] E. Beckman, *Science* **1999**, *283*, 946–947.
- [35] D. J. Darensbourg, M. W. Holtcamp, G. E. Struck, M. S. Zimmer, S. A. Niezgodna, P. Rainey, J. B. Robertson, J. D. Draper, J. H. Reibenspies, *J. Am. Chem. Soc.* **1999**, *121*, 107–116.
- [36] D. J. Darensbourg, J. R. Wildeson, J. C. Yarbrough, J. H. Reibenspies, *J. Am. Chem. Soc.* **2000**, *122*, 12487–12496.
- [37] M. Cheng, N. A. Darling, E. B. Lobkovsky, G. W. Coates, *Chem. Commun.* **2000**, 2007–2008.
- [38] M. Cheng, D. R. Moore, J. J. Reczek, B. M. Chamberlain, B. E. Lobkovsky, G. W. Coates, *J. Am. Chem. Soc.* **2001**, *123*, 8738–8749.
- [39] R. Eberhardt, M. Allmendinger, G. A. Luinstra, B. Rieger, *Organometallics* **2003**, *22*, 211–214.
- [40] D. J. Darensbourg, J. C. Yarbrough, C. Ortiz, C. C. Fang, *J. Am. Chem. Soc.* **2003**, *125*, 7586–7591.
- [41] F. Jutz, A. Buchard, M. R. Kember, S. B. Fredriksen, C. K. Williams, *J. Am. Chem. Soc.* **2011**, *133*, 17395–17405.
- [42] J. A. Castro-Osma, K. J. Lamb, M. North, *ACS Catal.* **2016**, *6*, 5012–5025.
- [43] F. Della Monica, B. Maity, T. Pehl, A. Buonerba, A. De Nisi, M. Monari, A. Grassi, B. Rieger, L. Cavallo, C. Capacchione, *ACS Catal.* **2018**, *8*, 6882–6893.
- [44] F. Della Monica, A. W. Kleij, *Catal. Sci. Technol.* **2020**, *10*, 3483–3501.
- [45] S. A. Kuznetsova, I. V. Gorodishch, A. S. Gak, V. V. Zherebtsova, I. S. Gerasimov, M. G. Medvedev, D. Kh Kitaeva, E. A. Khakina, M. North, Y. N. Belokon, *Tetrahedron* **2021**, *82*, 131929.
- [46] B. K. Muñoz, M. Viciano, C. Godard, S. Castellón, M. García-Ruiz, M. D. Blanco González, C. Claver, *Inorg. Chim. Acta* **2021**, *517*, 120194.
- [47] M. A. Emelyanov, N. V. Stoletova, A. A. Lisov, M. G. Medvedev, A. F. Smol'yakov, V. I. Maleev, V. A. Larionov, *Inorg. Chem. Front.* **2021**, *8*, 3871–3884.
- [48] A. Vidal-López, S. Posada-Pérez, M. Solà, V. D'Elia, A. Poater, *Green Chem.* **2022**, *3*, 180–187.
- [49] H.-Q. Yang, Z.-X. Chen, *J. Mol. Catal.* **2021**, *511*, 111733.
- [50] H. Wang, L. Guo, *ChemistrySelect* **2020**, *5*, 2516–2521.
- [51] J. Cheng, C. Lu, B. Zhao, *New J. Chem.* **2021**, *45*, 13096–13103.
- [52] X. He, Y. Wang, D. Yuan, H. You, Y. Yao, *Inorg. Chem.* **2021**, *60*, 11521–11529.
- [53] S. Saltarini, N. Villegas-Escobar, J. Martínez, C. G. Daniliuc, R. A. Matute, L. H. Gade, R. S. Rojas, *Inorg. Chem.* **2021**, *60*, 1172–1182.
- [54] E. Y. Seong, J. H. Kim, N. H. Kim, K.-H. Ahn, E. J. Kang, *ChemSusChem* **2019**, *12*, 409–415.
- [55] J. H. Kim, S. H. Lee, N. H. Kim, E. J. Kang, *J. CO<sub>2</sub> Util.* **2021**, *50*, 101595.
- [56] R. Luo, M. Chen, F. Zhou, J. Zhan, Q. Deng, Y. Yu, Y. Zhang, W. Xu, Y. Fang, *J. Mater. Chem. A* **2021**, *9*, 25731–25749.
- [57] J. P. S. C. Leal, W. A. Bezerra, R. P. das Chagas, C. H. J. Franco, F. T. Martins, A. M. Meireles, F. C. T. Antonio, P. Homem-de-Mello, T. T. Tasso, J. L. S. Milani, *Inorg. Chem.* **2021**, *60*, 12263–12273.
- [58] N. Panza, A. di Biase, E. Gallo, A. Caselli, *J. CO<sub>2</sub> Util.* **2021**, *51*, 101635.
- [59] M. R. Kember, C. K. Williams, *J. Am. Chem. Soc.* **2012**, *134*, 15676–15679.
- [60] M. R. Kember, P. D. Knight, P. T. R. Reung, C. K. Williams, *Angew. Chem. Int. Ed.* **2009**, *121*, 949–951.
- [61] M. R. Kember, A. J. P. White, C. K. Williams, *Inorg. Chem.* **2009**, *48*, 9535–9542.
- [62] A. Buchard, M. R. Kember, K. G. Sandeman, C. K. Williams, *Chem. Commun.* **2011**, *47*, 212–214.
- [63] V. Paradiso, V. Capaccio, D. H. Lamparelli, C. Capacchione, *Coord. Chem. Rev.* **2021**, *429*, 213644.
- [64] J. Chen, X. Wu, H. Ding, N. Liu, B. Liu, L. He, *ACS Sustainable Chem. Eng.* **2021**, *9*, 16210–16219.
- [65] A. Thevenon, A. Cyriac, D. Myers, A. J. P. White, C. B. Durr, C. K. Williams, *J. Am. Chem. Soc.* **2018**, *140*, 6893–6903.
- [66] Y. Reddi, C. J. Cramer, *ACS Catal.* **2021**, *11*, 15244–15251.
- [67] V. Paradiso, F. Della Monica, D. H. Lamparelli, S. D'Aniello, B. Rieger, C. Capacchione, *Catal. Sci. Technol.* **2021**, *11*, 4702–4707.
- [68] F. Della Monica, V. Paradiso, A. Grassi, S. Milione, L. Cavallo, C. Capacchione, *Chem. Eur. J.* **2020**, *26*, 5347–5353.
- [69] F. Niknam, V. Capaccio, M. Kleybolte, D. H. Lamparelli, M. Winnacker, G. Fiorani, C. Capacchione, *ChemPlusChem*, in press, DOI: 10.1002/cplu.202200038.
- [70] L. Qu, T. Roisnel, M. Cordier, D. Yuan, Y. Yao, B. Zhao, E. Kirillov, *Inorg. Chem.* **2020**, *59*, 16976–16987.
- [71] Q. Yao, Y. Chen, Y. Wang, D. Yuan, H. You, Y. Yao, *J. Rare Earth*, in press, DOI: 10.1016/j.jre.2021.07.007.
- [72] S. K. Raman, A. C. Deacy, L. Pena Carrodegua, N. V. Reis, R. W. F. Kerr, A. Phanopoulos, S. Morton, M. G. Davidson, C. K. Williams, *Organometallics* **2020**, *39*, 1619–1627.
- [73] T. Ema, Y. Miyazaki, J. Shimonishi, C. Maeda, J.-Y. Hasegawa, *J. Am. Chem. Soc.* **2014**, *136*, 15270–15279.
- [74] T. Ema, Y. Miyazaki, S. Koyama, Y. Yano, T. Sakai, *Chem. Commun.* **2012**, *48*, 4489–4491.
- [75] T. Aida, M. Ishikawa, S. Inoue, *Macromolecules* **1986**, *19*, 8.
- [76] Y. S. Qin, L. J. Chen, X. H. Wang, X. J. Zhao, F. S. Wang, *Chin. J. Polym. Sci.* **2011**, *29*, 602.
- [77] W. Wu, X. F. Sheng, Y. S. Qin, L. J. Qiao, Y. Y. Miao, X. H. Wang, F. S. Wang, *J. Polym. Sci. Part A* **2014**, *52*, 2346.
- [78] T. Aida, S. Inoue, *J. Am. Chem. Soc.* **1983**, *105*, 1304–1309.
- [79] J. Deng, M. Ratanasak, Y. Sako, H. Tokuda, C. Maeda, J.-Y. Hasegawa, K. Nozaki, T. Ema, *Chem. Sci.* **2020**, *11*, 5669–5675.
- [80] G. Trott, P. K. Saini, C. K. Williams, *Phil. Trans. R. Soc. A* **2016**, *374*, 20150085.
- [81] T. Stöber, T. T. D. Chen, Y. Zhu, C. K. Williams, *Phil. Trans. R. Soc. A* **2017**, *376*, 20170066.
- [82] J. A. Garden, P. K. Saini, C. K. Williams, *J. Am. Chem. Soc.* **2015**, *137*, 15078–15081.
- [83] J. A. Garden, A. J. P. White, C. K. Williams, *Dalton Trans.* **2017**, *46*, 2532–2541.
- [84] A. C. Deacy, C. B. Durr, J. A. Garden, A. J. P. White, C. K. Williams, *Inorg. Chem.* **2018**, *57*, 15575–15583.
- [85] G. Trott, J. A. Garden, C. K. Williams, *Chem. Sci.* **2019**, *10*, 4618–4627.
- [86] A. C. Deacy, A. F. R. Kilpatrick, A. Regoutz, C. K. Williams, *Nat. Chem.* **2020**, *12*, 372–380.
- [87] A. C. Deacy, E. Moreby, A. Phanopoulos, C. K. Williams, *J. Am. Chem. Soc.* **2020**, *142*, 19150–19160.
- [88] W. Lindeboom, D. A. X. Fraser, C. B. Durr, C. K. Williams, *Chem. Eur. J.* **2021**, *27*, 12224–12231.
- [89] A. J. Plajer, C. K. Williams, *Angew. Chem. Int. Ed.* **2021**, *60*, 13372–13379.
- [90] A. J. Plajer, C. K. Williams, *ACS Catal.* **2021**, *11*, 14819–14828.
- [91] J. R. Pankhurst, S. Paul, Y. Zhu, C. K. Williams, J. B. Love, *Dalton Trans.* **2019**, *48*, 4887–4893.

Manuscript received: May 26, 2022  
 Revised manuscript received: June 27, 2022  
 Accepted manuscript online: July 5, 2022  
 Version of record online: July 27, 2022